

Molecular precursors of the RNA-world in space: new nitriles in the G+0.693-0.027 molecular cloud

Víctor M. Rivilla^{1,*}, Izaskun Jiménez-Serra¹, Jesús Martín-Pintado¹, Laura Colzi¹, Belén Tercero², Pablo de Vicente³, Shaoshan Zeng⁴, Sergio Martín^{5,6}, Juan García de la Concepción¹, Luca Bizzocchi⁷, Mattia Melosso^{7,8}, Fernando Rico-Villas¹, Miguel A. Requena-Torres^{9,10}

¹Centro de Astrobiología (CSIC-INTA), Ctra Ajalvir km 4, 28850, Torrejón de Ardoz, Madrid, Spain ²Observatorio Astronómico Nacional (OAN-IGN), Calle Alfonso XII, 3, 28014 Madrid, Spain ³Observatorio de Yebes (OY-IGN), Cerro de la Palera SN, Yebes, Guadalajara, Spain ⁴Star and Planet Formation Laboratory, Cluster for Pioneering Research, RIKEN, 2-1 Hirosawa, Wako, Saitama, 351-0198, Japan ⁵European Southern Observatory, ALMA Department of Science, Alonso de Córdova 3107, Vitacura 763 0355, Santiago, Chile ⁶Joint ALMA Observatory, Department of Science Operations, Alonso de Córdova 3107, Vitacura 763 0355, Santiago, Chile ⁷Department of Chemistry “Giacomo Ciamician”, University of Bologna, Via F. Selmi 2, Bologna, 40126, Italy ⁸Scuola Superiore Meridionale, Università di Napoli Federico II, Largo San Marcellino 10, Naples, 80138, Italy ⁹University of Maryland, Department of Astronomy, College Park, ND 20742-2421, USA ¹⁰Department of Physics, Astronomy and Geosciences, Towson University, Towson, MD 21252, USA

Correspondence*:
Corresponding Author
vrivilla@cab.inta-csic.es

ABSTRACT

Nitriles play a key role as molecular precursors in prebiotic experiments based on the RNA-world scenario for the origin of life. These chemical compounds could have been partially delivered to the young Earth from extraterrestrial objects, stressing the importance of establishing the reservoir of nitriles in the interstellar medium. We report here the detection towards the molecular cloud G+0.693-0.027 of several nitriles, including cyanic acid (HOCN), and three C₄H₃N isomers (cyanoallene, CH₂CCHCN; propargyl cyanide, HCCCH₂CN; and cyanopropyne (CH₃CCCN), and the tentative detections of cyanoformaldehyde (HCOCN), and glycolonitrile (HOCH₂CN). We have also performed the first interstellar search of cyanoacetaldehyde (HCOCH₂CN), which was not detected. Based on the derived molecular abundances of the different nitriles in G+0.693-0.027 and other interstellar sources, we have discussed their formation mechanisms in the ISM. We propose that the observed HOCN abundance in G+0.693-0.027 is mainly due to surface chemistry and subsequent shock-induced desorption, while HCOCN might be mainly formed through gas-phase chemistry. In the case of HOCH₂CN, several grain-surface routes from abundant precursors

could produce it. The derived abundances of the three C_4H_3N isomers in G+0.693-0.027 are very similar, and also similar to those previously reported in the dark cold cloud TMC-1. This suggests that the three isomers are likely formed through gas-phase chemistry from common precursors, possibly unsaturated hydrocarbons (CH_3CCH and CH_2CCH_2) that react with the cyanide radical (CN). The rich nitrile feedstock found towards G+0.693-0.027 confirms that interstellar chemistry is able to synthesize in space molecular species that could drive the prebiotic chemistry of the RNA-world.

Keywords: astrochemistry, Molecules - ISM, Molecular clouds, RNA-world, prebiotic chemistry

1 INTRODUCTION

Life on Earth appeared about 3.8 billion years ago, around 700 Myr after the formation of the planet (Pearce et al. 2018), but we still do not know the mechanisms that made it possible. One of the most supported hypotheses for the origin of life is known as the RNA world (Gilbert 1986), in which RNA could have performed both metabolic and genetic roles. The process by which inert matter generated first the building blocks of RNA, ribonucleotides, and ultimately RNA itself, remains a mystery. Recent laboratory experiments mimicking prebiotic conditions have shown that ribonucleotides could be synthesized starting from simple molecules (e.g. Powner et al. 2009; Patel et al. 2015; Becker et al. 2019). A plausible origin of this prebiotic material is extraterrestrial delivery (Oró 1961; Chyba and Sagan 1992; Cooper et al. 2001) during the heavy bombardment of meteorites and comets that occurred around 3.9 billions ago (Marchi et al. 2014). These basic molecular precursors may have been already formed prior to the formation of the Solar System, in its parental molecular cloud, through the chemistry that takes place in the interstellar medium (ISM). Therefore, the study of the molecular complexity of the ISM can provide us an illustrative view of the chemical reservoir that could have contributed to feed the prebiotic chemistry on the primitive Earth, and could potentially develop similar processes in other places in the Galaxy under favourable Earth-like planetary environments.

In the last decades, and especially in the last years, astrochemistry has shown that interstellar chemistry is able to synthesize building blocks of key biomolecules. Several of the precursors of ribonucleotides spotted by the prebiotic experiments in the laboratory have been detected in the ISM, like cyanoacetylene (HC_3N , Turner 1971), cyanamide (NH_2CN , Turner et al. 1975), glycolaldehyde (CH_2OHCHO , Hollis et al. 2004, urea (NH_2CONH_2 , Belloche et al. 2019), hydroxylamine (NH_2OH , Rivilla et al. 2020), and 1,2-ethenediol ($(CHOH)_2$; Rivilla et al. 2022a). Among the key simple molecular precursors required for the RNA world, numerous works have stressed the dominant role of a particular family of compounds, nitriles, which are molecules with the $C\equiv N$ moiety. This simple but highly versatile functional group offers a unique potential to build-up molecular complexity and activate efficiently the formation of ribonucleotides (Powner et al. 2009; Powner and Sutherland 2010; Patel et al. 2015; Mariani et al. 2018; Becker et al. 2019; Menor Salván et al. 2020), and also other key biomolecules such as peptides or nucleobases (Menor-Salván and Marín-Yaseli 2012; Canavelli et al. 2019; Foden et al. 2020).

With the aim of extending our knowledge on the chemistry of nitriles in the ISM, in this work we have searched for more nitriles towards the molecular cloud G+0.693-0.027 (hereafter G+0.693), including some with increasing complexity that have been proposed as important precursors of prebiotic chemistry. This cloud, located in the Sgr B2 region of the center of our Galaxy, is one of the most chemically rich sources in the ISM. Numerous nitrogen-bearing species, including nitriles, have been detected (see Zeng et al. 2018; Rivilla et al. 2019b, 2021b): cyanoacetylene (HC_3N), acetonitrile (CH_3CN), cyanamide (NH_2CN), the cyanomethyl radical (H_2CCN), cyanomethanimine ($HNCHCN$), and the cyanomidyl radical ($HNCN$).

In this work we report the detection of cyanic acid (HOCN), the tentative detections of glycolonitrile (HOCH₂CN) and cyanoformaldehyde (HCOCN), and the first interstellar search of cyanoacetaldehyde (HCOCH₂CN) in the ISM, for which we provide an abundance upper limit. We have also searched for three unsaturated carbon-chain nitriles, the C₄H₃N isomers. We report the detection of cyanopropyne (CH₃CCCN), and the second detections in the ISM of cyanoallene (CH₂CCHCN) and propargyl cyanide (HCCCH₂CN), detected previously only towards the TMC-1 dark cloud (Lovas et al. 2006; McGuire et al. 2020; Marcelino et al. 2021). In Section 2 we present the data of the observational survey, in Section 3 we describe the line identification and analysis, and present the results of the line fitting, and in Section 4 we discuss about the interstellar chemistry of the different species and their possible roles in prebiotic chemistry.

2 OBSERVATIONS

A high sensitivity spectral survey was carried out towards G+0.693. We used both IRAM 30m telescope (Granada, Spain) and Yebes 40m telescope (Guadalajara, Spain). The observations were centred at $\alpha(\text{J2000.0}) = 17^{\text{h}}47^{\text{m}}22^{\text{s}}$, and $\delta(\text{J2000.0}) = -28^{\circ}21'27''$. The position switching mode was used in all the observations with the off position located at $\Delta\alpha = -885''$, $\Delta\delta = 290''$ from the source position. During the IRAM 30m observations the dual polarisation receiver EMIR was connected to the fast Fourier transform spectrometers (FFTS), which provided a channel width of 200 kHz. In this work we have used data covering the spectral windows from 71.8 to 116.7 GHz, 124.8 to 175.5 GHz, and 199.8–238.3 GHz. The spectra were smoothed to velocity resolutions of 1.0–2.6 km s⁻¹, depending on the frequency. The observations with the Yebes 40m radiotelescope used the Nanocosmos Q-band (7 mm) HEMT receiver (Tercero et al. 2021). The receiver was connected to 16 FFTS providing a channel width of 38 kHz and a bandwidth of 18.5 GHz per polarisation, covering the frequency range between 31.3 GHz and 50.6 GHz. The spectra were smoothed to a resolution of 251 kHz, corresponding to velocity resolutions of 1.5–2.4 km s⁻¹. The noise of the spectra depends on the frequency range, with values in antenna temperature (T_{A}^*) as low as 1.0 mK, while in some intervals it increases up to 4.0–5.0 mK, for the Yebes data, and 1.3 to 2.8 mK (71–90 GHz), 1.5 to 5.8 mK (90–115 GHz), ~ 10 mK (115–116 GHz), 3.1 to 6.8 mK (124–175 GHz), and 4.5 to 10.6 mK (199–238 GHz), for the IRAM 30m data. The line intensity of the spectra was measured in units of T_{A}^* as the molecular emission toward G+0.693 is extended over the beam (Requena-Torres et al. 2006, 2008; Zeng et al. 2018, 2020).

3 ANALYSIS AND RESULTS

Figure 1 shows the nitriles analysed in this work, which include four oxygen-bearing nitriles: cyanic acid (HOCN), cyanoformaldehyde (or formyl cyanide, HCOCN), glycolonitrile (or 2-hydroxyacetonitrile, HCOCH₂CN), cyanoacetaldehyde (or 3-oxopropanenitrile, HCOCH₂CN); and three C₄H₃N isomers: cyanoallene (or 2,3-butadienenitrile, CH₂CCHCN), propargyl cyanide (or 3-butyne nitrile, HCCCH₂CN), and cyanopropyne (or 2-butyne nitrile, CH₃CCCN). The identification and fitting of the molecular lines were performed using the SLIM (Spectral Line Identification and Modeling) tool within the MADCUBA package¹ (version 09/11/2021; Martín et al. 2019). SLIM generates synthetic spectra under the assumption of Local Thermodynamic Equilibrium (LTE), using the spectroscopy provided by laboratory experiments assisted by theoretical calculations. Table 1 lists the spectroscopic references of all the molecules analysed. We have used entries from the Cologne Database for Molecular Spectroscopy (CDMS, Endres et al. 2016), which are based on the laboratory works and theoretical calculations indicated in Table 1. Moreover, we implemented into MADCUBA the spectroscopy of HCOCH₂CN from Møllendal et al. (2012).

¹ Madrid Data Cube Analysis on ImageJ is a software developed at the Center of Astrobiology (CAB) in Madrid; <https://cab.inta-csic.es/madcuba/>

Table 1. Spectroscopy of the molecules analysed in this work. The molecular catalog, number and date of the entry, and the references for the line lists and dipole moments are listed.

Molecule	Catalog	Entry	Date	Line list ref.	Dipole moment ref.
HOCN	CDMS	43510	May 2009	Brünken et al. (2009)	Brünken et al. (2009)
HCOCN	CDMS	55501	June 2006	Bogey et al. (1995)	Császár 1989
HOCH ₂ CN	CDMS	57512	March 2017	Margulès et al. (2017)	Margulès et al. (2017)
HCOCH ₂ CN	MADCUBA	–	January 2022	Møllendal et al. (2012)	Møllendal et al. (2012)
HCCCH ₂ CN	CDMS	65514	September 2020	Demaison et al. (1985) McGuire et al. (2020)	Demaison et al. (1985)
CH ₂ CCHCN	CDMS	65506	March 2006	Bouchy et al. (1973) Schwahn et al. (1986)	Bouchy et al. (1973)
CH ₃ CCCN	CDMS	65503	April 2004	Moïses et al. (1982), Bester et al. (1983)	Bester et al. (1984)

To evaluate if the molecular transitions of interest are blended with emission from other species, we have also considered the LTE model that includes the total contribution of all the species that have been identified so far towards G+0.693 (e.g., Requena-Torres et al. 2008; Zeng et al. 2018; Rivilla et al. 2019a, 2020; Jiménez-Serra et al. 2020; Rivilla et al. 2021a,b; Zeng et al. 2021; Rodríguez-Almeida et al. 2021a,b; Rivilla et al. 2022a,b). To derive the physical parameters of the molecular emission, we used the AUTOFIT tool of SLIM, which finds the best agreement between the observed spectra and the predicted LTE model, and provides the best solution for the parameters, and their associated uncertainties (see details of the formalism used in Martín et al. 2019). The free parameters of the model are: molecular column density (N), excitation temperature (T_{ex}), linewidth (or full width at half maximum, FWHM), and velocity (v_{LSR}). We have left these four parameters free whenever possible, providing their associated uncertainties. For the cases in which the algorithm used by AUTOFIT does not converge, we have fixed some of them to allow the algorithm to converge. In the following, we present the analysis of the different molecules studied. For each species, we have applied AUTOFIT using unblended transitions and transitions that, while partially blended with other species already identified in G+0.693, properly reproduces the observed spectra. We note that for all molecules the transitions that are not shown are consistent with the observed spectra, but they are heavily blended with lines from other molecular species or they are too weak to be detected, according to the line intensities predicted by the LTE model.

3.1 Oxygen-bearing nitriles

3.1.1 Cyanic acid (HOCN) and cyanoformaldehyde (HCOCN)

HOCN was already reported towards G+0.693 by Brünken et al. (2010) (their source Sgr B2 (20,100)²), and also by Zeng et al. (2018) using in both cases less sensitive observations. We provide here a new analysis using deeper observations. We have detected six transitions of this species that are completely unblended, which are shown in Figure 2, and listed in Table 2. These transitions include the three transitions identified by Zeng et al. (2018), the confirmation of the $8_{0,8}-7_{0,7}$ transition tentatively detected in that work (see their Figure B15), and two new transitions (Table 2). The best LTE fit derived by MADCUBA, where all parameters were left free, is shown in Figure 2, and the derived physical parameters are presented in Table 4. We obtained a column density of $(2.13 \pm 0.04) \times 10^{13} \text{ cm}^{-2}$ (Table 4), which translates into a molecular abundance with respect to molecular hydrogen of 1.6×10^{-10} , using $N_{\text{H}_2} = 1.35 \times 10^{23} \text{ cm}^{-2}$

² The position of this source is offset in (α, δ) by $(20'', 100'')$ with respect to that of Sgr B2(M), see Brünken et al. (2010).

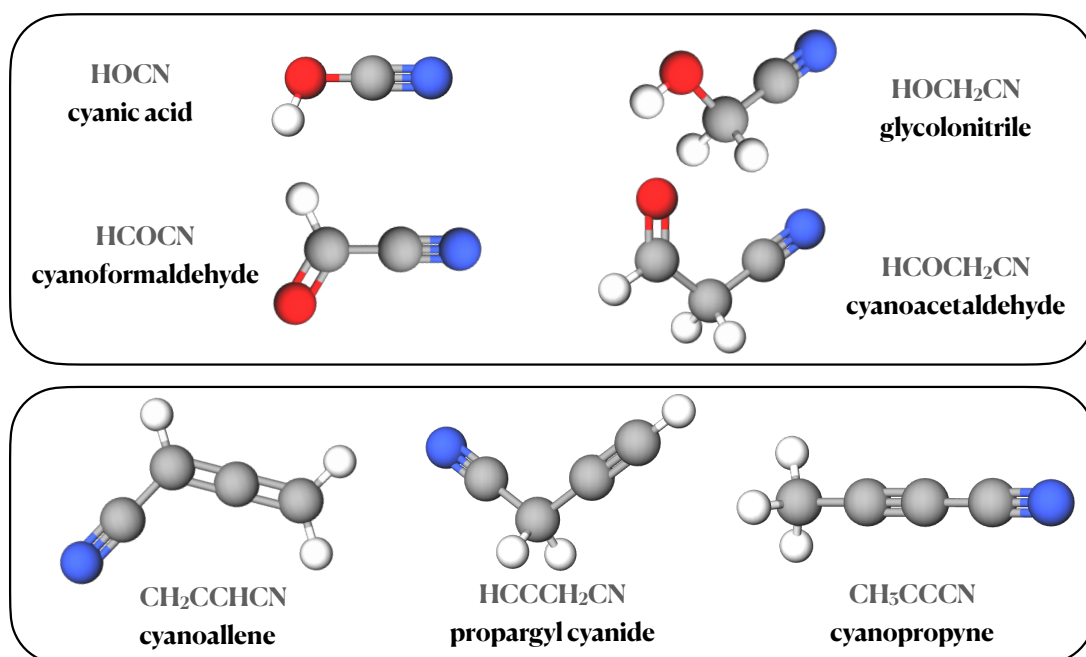


Figure 1. Three-dimensional representation of the oxygen-bearing nitriles (upper panel) and the three C₄H₃N isomers (lower panel) analysed in this work. White, gray, red, and blue corresponds to hydrogen, carbon, oxygen and nitrogen atoms, respectively.

from Martín et al. (2008). The results are consistent, within the uncertainties, with those derived by Zeng et al. (2018).

We also report here the first tentative detection of HCOCN towards G+0.693. Figure 3 shows that the $3_{1,3}-2_{0,2}$ (90.5710141 GHz) and $4_{1,4}-3_{0,3}$ (99.5348108 GHz) transitions are unblended, while other transitions are partially blended with other species (Table 2). To perform the fit, we fixed T_{ex} , FWHM, and v_{LSR} to the ones derived from HOCN. We obtained a column density of $(0.76 \pm 0.11) \times 10^{13} \text{ cm}^{-2}$, almost one order of magnitude lower than the upper limit reported by Zeng et al. (2018) of $< 6 \times 10^{13} \text{ cm}^{-2}$ towards G+0.693. The derived molecular abundance is 6×10^{-11} , which is very similar to that found in the TMC-1 dark cloud by Cernicharo et al. (2021). The HOCN/HCOCN ratio is ~ 2.8 .

3.1.2 Glycolonitrile (HOCH₂CN)

This species is also tentatively detected towards G+0.693. We show in Figure 4 two molecular transitions of HOCH₂CN that are unblended (Table 2), and those partially blended with other species already identified in this cloud. To perform the fit, we fixed T_{ex} and FWHM to the ones derived for HOCN, and used $v_{\text{LSR}} = 67 \text{ km s}^{-1}$, which best reproduces the velocity of the two unblended transitions. We obtained a column density of $(0.8 \pm 0.2) \times 10^{13} \text{ cm}^{-2}$ (Table 4), and a molecular abundance of 6×10^{-11} , very similar to that of HOCN.

Table 2. List of detected transitions of the oxygen-bearing nitriles analysed in this work. We indicate the frequency, quantum numbers, logarithm of the Einstein coefficient (A_{ul}), energy of the upper levels of each transition (E_u), and information about the possible blending by other identified or unidentified (U) species towards G+0.693.

Molecule	Frequency (GHz)	Transition J_{K_a, K_c}	$\log A_{ul}$ (s^{-1})	E_u (K)	Blending
HOCN	41.9508371	$2_{0,2}-1_{0,1}$	-5.3239	3.0	unblended
HOCN	83.5383960	$4_{1,4}-3_{1,3}$	-4.4087	42.2	blended with U
HOCN	83.9005702 ^a	$4_{0,4}-3_{0,3}$	-4.3750	10.1	unblended
HOCN	84.2524547	$4_{1,3}-3_{1,2}$	-4.3976	42.3	blended with HCCCH ₂ CN
HOCN	104.8746777 ^a	$5_{0,5}-4_{0,4}$	-4.0746	15.1	unblended
HOCN	125.8480951	$6_{0,6}-5_{0,5}$	-3.8304	21.1	unblended
HOCN	146.8206846 ^a	$7_{0,7}-6_{0,6}$	-3.6248	28.1	unblended
HOCN	167.7923140 ^b	$8_{0,8}-7_{0,7}$	-3.4472	36.2	unblended
HCOCN	72.1192555	$1_{1,1}-0_{0,0}$	-5.0767	3.5	blended
HCOCN	81.433113	$2_{1,2}-1_{0,1}$	-4.9642	4.4	blended with NH ₂ CH ₂ CH ₂ OH
HCOCN	90.5710141	$3_{1,3}-2_{0,2}$	-4.8461	5.7	unblended
HCOCN	99.5348108	$4_{1,4}-3_{0,3}$	-4.7342	7.6	unblended
HCOCN	108.3274964	$5_{1,5}-4_{0,4}$	-4.6301	9.8	part. blended with HCCO and U
HCOCN	207.3132961	$2_{2,0}-1_{1,1}$	-3.7478	13.4	blended with U
HOCH ₂ CN	35.934379	$4_{1,4}-3_{1,3}$	-5.8654	5.7	unblended
HOCH ₂ CN	37.781601	$4_{1,3}-3_{1,2}$	-5.8001	5.9	blended with <i>c</i> -C ₂ H ₄ O and U
HOCH ₂ CN	44.907438	$5_{1,5}-4_{1,4}$	-5.5549	7.9	blended with <i>t</i> -HCOOH
HOCH ₂ CN	45.975528	$5_{0,5}-4_{0,4}$	-5.5069	6.6	unblended
HOCH ₂ CN	75.463333	$8_{1,7}-7_{1,6}$	-4.8528	17.7	blended with <i>s</i> -C ₂ H ₅ CHO

(a) Transition detected in Zeng et al. (2018).

(b) Transition tentatively detected in Zeng et al. (2018).

3.1.3 Cyanoacetaldehyde (HCOCH₂CN)

This molecule is not currently included in any of the commonly used molecular databases such as CDMS or the Jet Propulsion Laboratory catalog (JPL; Pickett et al. 1998). The conformational energy landscape of HCOCH₂CN and the effects of the large amplitude motions on its rotational spectrum have been described in detail by Møllendal et al. (2012). We have used the spectroscopic information provided in this work to implement it into MADCUBA. The most stable rotamer (referred to as species I in the cited reference) possesses two equivalent positions in the electronic energy potential function for rotation about its C₁–C₂ bond (see figure 1 of Møllendal et al. 2012). They are separated by a barrier of 0.84 kJ mol⁻¹ (computed at MP2 level) at the exact antiperiplanar conformation. Large amplitude vibrations and tunneling for the torsion about the C₁–C₂ bond leads to the existence of two closely spaced energy levels for the ground state labelled with a plus sign (+) for the lowest-energy level and with a minus sign (–) for the higher-energy level. These two states are separated by an energy difference $\Delta E/h$ of ~ 58.8 GHz. For the present spectral calculation we have reanalysed the rotational transitions reported by Møllendal et al. (2012) using the same set of spectroscopic parameters employed in their fit 1 (see their Table 4). The rest-frequencies have then been computed in the $J=0-70$ interval with $K_{a,max} = 50$. Theoretical values of dipole moments $\mu_a = 0.932$ D, $\mu_b = 1.574$ D, and $\mu_c = 1.274$ D, computed at CCSD level (Møllendal et al., 2012) have been employed. All the calculations have been performed with the CALPGM suite of programs Pickett (1991).

This species is not detected towards G+0.693. We have derived an upper limit for its abundance using the brightest transition according to the LTE model that are unblended, namely the $6_{2,5}-5_{1,4}$ transition at 101.598576 GHz. MADCUBA calculates the upper limit of the column density using the 3σ value of the

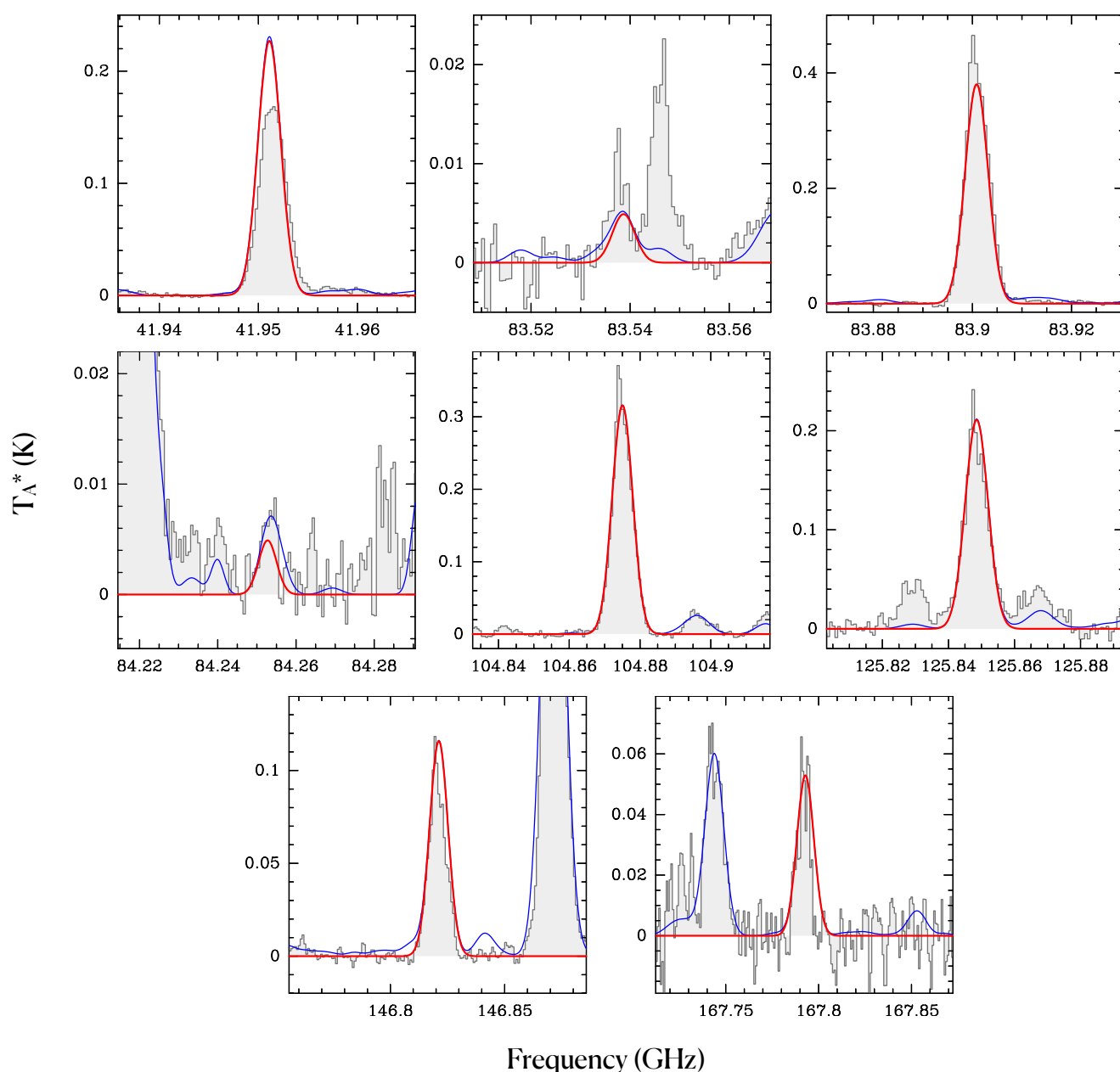


Figure 2. Selected cyanic acid (HOCN) transitions (see Table 2) detected towards the G+0.693 molecular cloud. The best LTE fit derived with MADCUBA for the HOCN emission is shown with a red curve, while the blue curve shows the total emission considering all the species identified towards this molecular cloud. The y-axis shows the line intensity in antenna temperature scale (T_A^*) in Kelvin, and the x-axis shows the frequency in GHz.

integrated intensity (see details in Martín et al. 2019). We have used the same T_{ex} , FWHM, and v_{LSR} used for HOCH₂CN. We obtained an upper limit of the HCOCH₂CN abundance of $<2.7 \times 10^{-10}$ (Table 4).

3.2 C₄H₃N isomers

We report in this section the first detection towards G+0.693 of cyanoallene (CH₂CCHCN), propargyl cyanide (HCCCH₂CN), and cyanopropyne (CH₃CCCN).

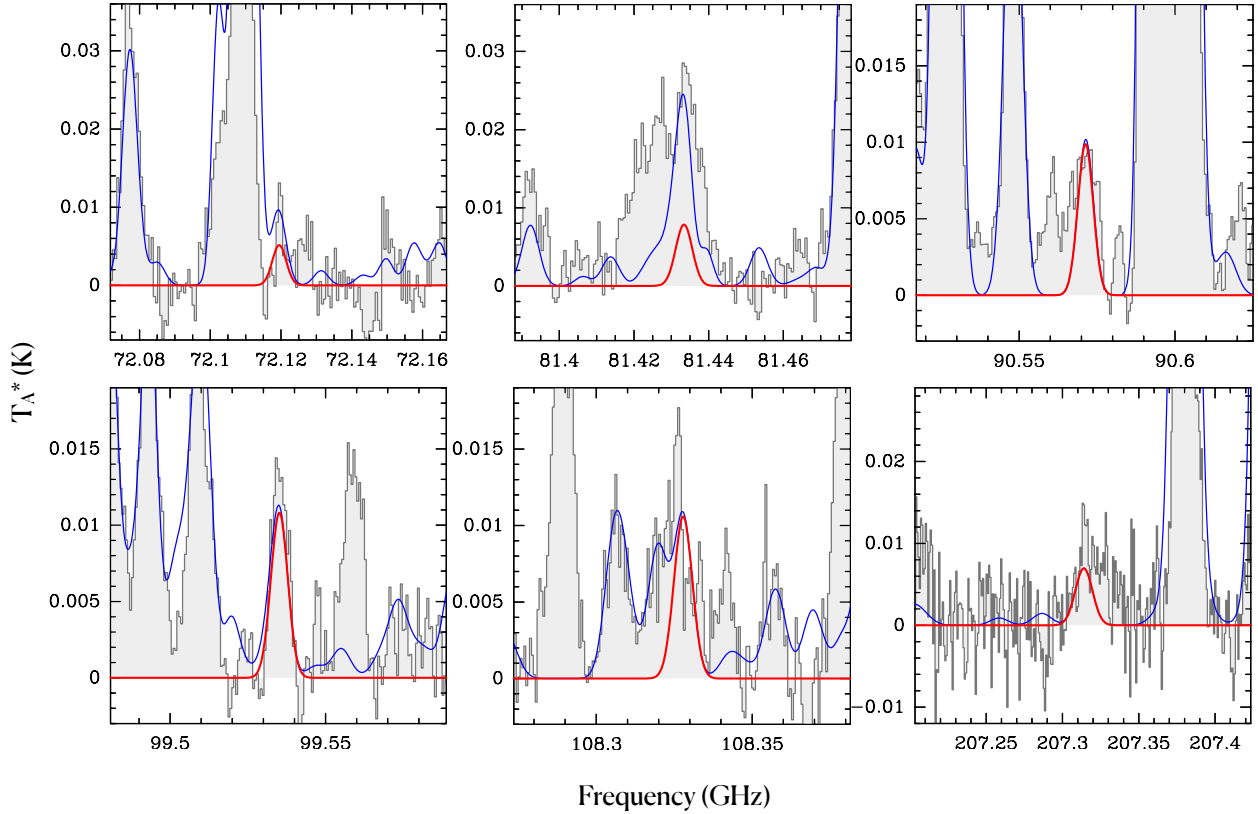


Figure 3. Selected cyanoformaldehyde (HCOCN) transitions (see Table 2) detected towards the G+0.693 molecular cloud. The best LTE fit derived with MADCUBA for the HCOCN emission is shown with a red curve, while the blue curve shows the total emission considering all the species identified towards this molecular cloud. The y-axis shows the line intensity in antenna temperature scale (T_A^*) in Kelvin, and the x-axis shows the frequency in GHz.

3.2.1 Cyanoallene (CH_2CCHCN)

Figure 5 shows the molecular transitions of CH_2CCHCN that are unblended, or only slightly blended with other species already identified in this source, whose spectroscopic information is presented in Table 3. The G+0.693 cloud is the second interstellar source where CH_2CCHCN has been detected, after the cold cloud TMC-1 (Lovas et al. 2006; Marcelino et al. 2021). We left N , T_{ex} , FWHM, and v_{LSR} as free parameters, and obtained a column density of $(2.34 \pm 0.06) \times 10^{13} \text{ cm}^{-2}$, and a molecular abundance of 1.7×10^{-10} (Table 4).

3.2.2 Propargyl cyanide (HCCCH_2CN)

Figure 6 shows the molecular transitions of HCCCH_2CN that are unblended, or only slightly blended with other species already identified in this cloud, whose spectroscopic information is presented in Table 3. As in the case of its isomer CH_2CCHCN , G+0.693 is the second interstellar source where HCCCH_2CN has been detected, after the cold cloud TMC-1 (McGuire et al. 2020; Marcelino et al. 2021). We fixed T_{ex} and FWHM to the values obtained for CH_2CCHCN , and left N and v_{LSR} free. We obtained a column density of $(1.77 \pm 0.08) \times 10^{13} \text{ cm}^{-2}$, and a molecular abundance of 1.3×10^{-10} . The $\text{CH}_2\text{CCHCN}/\text{HCCCH}_2\text{CN}$ ratio is ~ 1.3 .

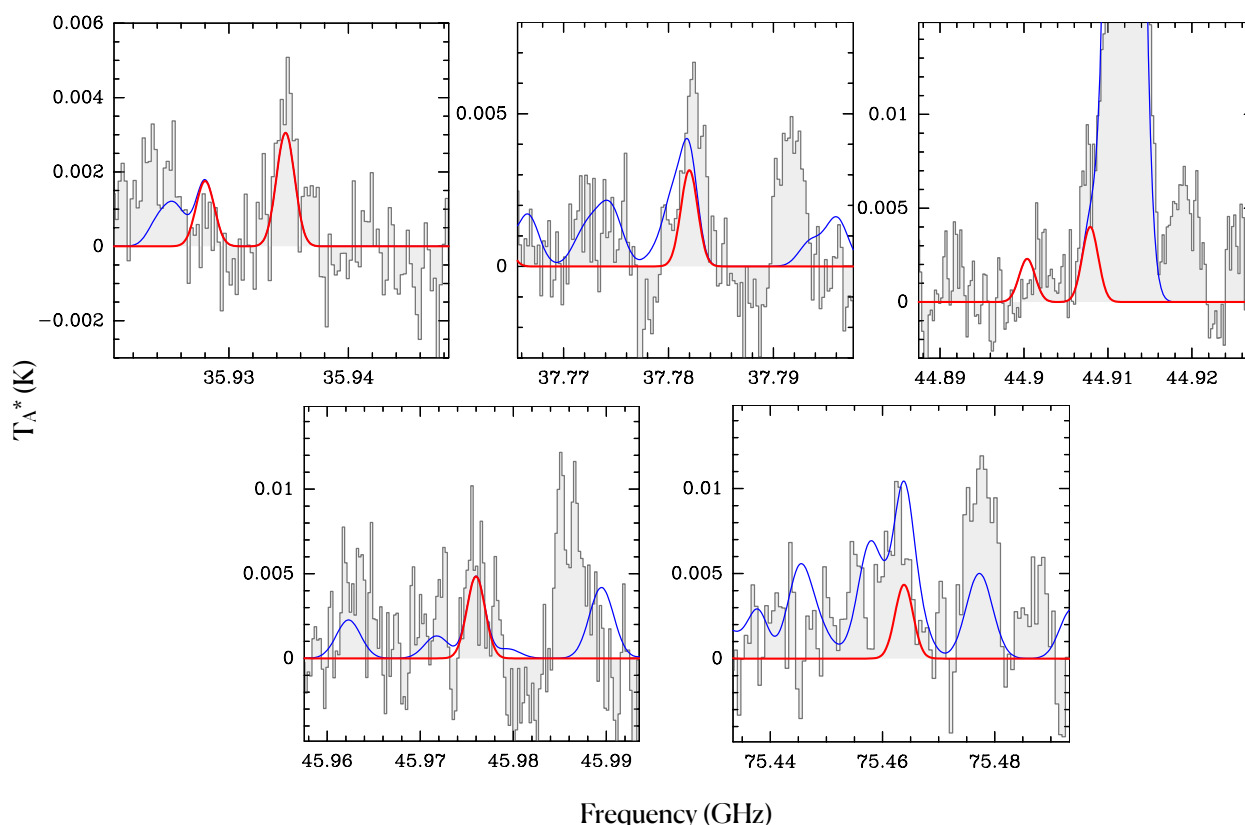


Figure 4. Selected transitions of glycolonitrile (HOCH_2CN ; see Table 2) detected towards the G+0.693 molecular cloud. The best LTE fit derived with MADCUBA for the HOCH_2CN emission is shown with a red curve, while the blue curve shows the total emission considering all the species identified towards this molecular cloud. The y-axis shows the line intensity in antenna temperature scale (T_A^*) in Kelvin, and the x-axis shows the frequency in GHz.

Table 3 . List of observed transitions of the $\text{C}_4\text{H}_3\text{N}$ isomers analysed in this work. We indicate the frequency, quantum numbers, Einstein coefficient (A_{ul}), energy of the upper levels of each transition (E_u), and information about the possible blending by other identified or unidentified (U) species towards G+0.693.

Molecule	Frequency (GHz)	Transition ^a	$\log A_{ul}$ (s^{-1})	E_u (K)	Blending
CH_2CCHCN	31.6156000	$6_{1,5}-5_{1,4}$	-5.5633	6.4	blended with $aGg'-(\text{CH}_2\text{OH})_2$
CH_2CCHCN	35.3790500	$7_{1,7}-6_{1,6}$	-5.4086	7.9	blended with CH_3COCH_3
CH_2CCHCN	36.0646889	$7_{0,7}-6_{0,6}$	-5.3748	6.9	unblended
CH_2CCHCN	36.1402200	$7_{2,6}-6_{2,5}$	-5.4089	11.4	unblended
CH_2CCHCN	36.2225000	$7_{2,5}-6_{2,4}$	-5.4059	11.4	unblended
CH_2CCHCN	36.8784700	$7_{1,6}-6_{1,5}$	-5.3546	8.2	blended with U
CH_2CCHCN	40.4257132	$8_{1,8}-7_{1,7}$	-5.2292	9.9	unblended
CH_2CCHCN	41.1870836	$8_{0,8}-7_{0,7}$	-5.1981	8.9	unblended
CH_2CCHCN	41.2976561	$8_{2,7}-7_{2,6}$	-5.2225	13.4	unblended
CH_2CCHCN	41.4207138	$8_{2,6}-7_{2,5}$	-5.2187	13.4	unblended
CH_2CCHCN	42.1384521	$8_{1,7}-7_{1,6}$	-5.1751	10.2	blended with $c\text{-C}_3\text{H}_2$
CH_2CCHCN	45.4695206	$9_{1,9}-8_{1,8}$	-5.0716	12.0	blended with CH_3NHCHO

Table 3 . Continued.

Molecule	Frequency (GHz)	Transition ^a	$\log A_{ul}$ (s ⁻¹)	E _u (K)	Blending
CH ₂ CCHCN	46.2978836	9 _{0,9} –8 _{0,8}	-5.0429	11.1	unblended
CH ₂ CCHCN	46.4528399	9 _{2,8} –8 _{2,7}	-5.0603	15.6	blended with CH ₃ CONH ₂
CH ₂ CCHCN	46.6280696	9 _{2,7} –8 _{2,6}	-5.0555	15.7	blended with HC ₂ CHO
CH ₂ CCHCN	47.3948488	9 _{1,8} –8 _{1,7}	-5.0176	12.5	unblended
CH ₂ CCHCN	75.6463060	7 _{3,4} –8 _{2,7}	-6.2551	17.0	blended with U
CH ₂ CCHCN	75.6587572	15 _{1,15} –14 _{1,14}	-4.3956	30.2	blended with U
CH ₂ CCHCN	76.6665519	15 _{0,15} –14 _{0,14}	-4.3767	29.6	blended with C ₂ H ₅ OH
CH ₂ CCHCN	78.0996741	15 _{2,13} –14 _{2,12}	-4.3600	34.4	blended with U
CH ₂ CCHCN	78.8285795	15 _{1,14} –14 _{1,13}	-4.3421	31.4	blended with CH ₃ COOH
CH ₂ CCHCN	81.674936	16 _{0,16} –15 _{0,15}	-4.2935	33.5	blended with C ₂ H ₅ OH
CH ₂ CCHCN	84.0442448	16 _{1,15} –15 _{1,14}	-4.2576	35.5	unblended
HCCCH ₂ CN	31.8489874	6 _{1,6} –5 _{1,5}	-5.2773	6.2	unblended
HCCCH ₂ CN	33.8637212	6 _{1,5} –5 _{1,4}	-5.1974	6.5	unblended
HCCCH ₂ CN	37.1392132	7 _{1,7} –6 _{1,6}	-5.0691	8.0	unblended
HCCCH ₂ CN	38.1027037	7 _{0,7} –6 _{0,6}	-5.0271	7.3	unblended
HCCCH ₂ CN	38.3423461	7 _{2,6} –6 _{2,5}	-5.0555	10.6	unblended
HCCCH ₂ CN	38.6167091	7 _{2,5} –6 _{2,4}	-5.0461	10.7	unblended
HCCCH ₂ CN	39.4865865	7 _{1,6} –6 _{1,5}	-4.9892	8.4	unblended
HCCCH ₂ CN	42.0111351	5 _{1,5} –4 _{0,4}	-5.4001	4.6	blended with n-C ₃ H ₇ CN
HCCCH ₂ CN	42.4217854	8 _{1,8} –7 _{1,7}	-4.8900	10.0	unblended
HCCCH ₂ CN	43.8024266	8 _{2,7} –7 _{2,6}	-4.8695	12.7	blended with HNCO
HCCCH ₂ CN	44.2102030	8 _{2,6} –7 _{2,5}	-4.8574	12.8	unblended
HCCCH ₂ CN	45.0990808	8 _{1,7} –7 _{1,6}	-4.8103	10.6	unblended
CH ₃ C ₃ N	33.0513004	8 ₁ –7 ₁	-5.3573	14.6	unblended
CH ₃ C ₃ N	33.0516190	8 ₀ –7 ₀	-5.3505	7.1	
CH ₃ C ₃ N	37.1826557	9 ₁ –8 ₁	-5.1995	16.4	blended with CH ₃ OCHO
CH ₃ C ₃ N	37.1830142	9 ₀ –8 ₀	-5.1942	8.9	
CH ₃ C ₃ N	41.3139909	10 ₁ –9 ₁	-5.0590	18.4	blended with <i>aGg'</i> -(CH ₂ OH) ₂
CH ₃ C ₃ N	41.3143891	10 ₀ –9 ₀	-5.0546	10.9	
CH ₃ C ₃ N	45.4453036	11 ₁ –10 ₁	-4.9321	20.6	unblended
CH ₃ C ₃ N	45.4457416	11 ₀ –10 ₀	-4.9286	13.1	
CH ₃ C ₃ N	49.5765916	12 ₁ –11 ₁	-4.8166	23.0	unblended
CH ₃ C ₃ N	49.5770694	12 ₀ –11 ₀	-4.8136	15.5	
CH ₃ C ₃ N	74.3636580	18 ₁ –17 ₁	-4.2809	41.4	unblended
CH ₃ C ₃ N	74.3643850	18 ₀ –17 ₀	-4.2795	33.9	
CH ₃ C ₃ N	82.6257600	20 ₁ –19 ₁	-4.1422	49.1	blended with <i>s</i> -C ₂ H ₅ CHO
CH ₃ C ₃ N	82.6265180	20 ₀ –19 ₀	-4.1411	41.6	
CH ₃ C ₃ N	86.756698	21 ₁ –20 ₁	-4.0780	53.3	blended with H ¹³ CO ⁺
CH ₃ C ₃ N	86.757524	21 ₀ –20 ₀	-4.0770	45.8	
CH ₃ C ₃ N	90.8876208	22 ₁ –21 ₁	-4.0169	57.7	blended with CH ₃ COCH ₃
CH ₃ C ₃ N	90.8884956	22 ₀ –21 ₀	-4.0159	50.2	
CH ₃ C ₃ N	95.0184892	23 ₁ –22 ₁	-3.9584	62.2	unblended

Table 3 . Continued.

Molecule	Frequency (GHz)	Transition ^a	$\log A_{ul}$ (s ⁻¹)	E _u (K)	Blending
CH ₃ C ₃ N	95.0194037	23 ₀ –22 ₀	-3.9576	54.7	unblended
CH ₃ C ₃ N	99.1493060	24 ₁ –23 ₁	-3.9026	67.0	
CH ₃ C ₃ N	99.1502601	24 ₀ –23 ₀	-3.9017	59.5	
CH ₃ C ₃ N	103.280069	25 ₁ –24 ₁	-3.8490	71.9	unblended
CH ₃ C ₃ N	103.2810626	25 ₀ –24 ₀	-3.8482	64.4	
CH ₃ C ₃ N	107.4107758	26 ₁ –25 ₁	-3.7975	77.1	blended with CH ₃ CONH ₂
CH ₃ C ₃ N	107.4118089	26 ₀ –25 ₀	-3.7968	69.6	

^a The format of the quantum numbers is J_{K_a, K_c} for HCCCH₂CN and CH₂CCHCN (asymmetric rotors), and J_K for CH₃C₃N (symmetric top molecule).

3.2.3 Cyanopropyne (CH₃CCCN)

Figure 7 shows the spectra of multiple unblended or slightly blended transitions of CH₃CCCN (listed in Table 3). Unlike its isomers, which are asymmetric molecules, CH₃CCCN is a symmetric top molecule. For the analysis, we have used the lowest energy $K=0$ and $K=1$ transitions (see Table 3), which are the ones that dominate the line emission in a source with low T_{ex} like G+0.693 (5–20 K; see e.g. Zeng et al. 2018). We fixed the FWHM and v_{LSR} to the values derived for CH₂CCHCN, leaving N and T_{ex} as free parameters. We obtained a column density of $(1.35 \pm 0.03) \times 10^{13} \text{ cm}^{-2}$ (Table 4), and a molecular abundance of 1.0×10^{-10} . The isomeric ratios of CH₂CCHCN/CH₃CCCN and HCCCH₂CN/CH₃CCCN are ~ 1.8 and ~ 1.3 , respectively.

4 DISCUSSION

4.1 Interstellar chemistry

4.1.1 Oxygen-bearing nitriles

We show in Figure 8 the molecular abundances of the O-bearing nitriles detected towards G+0.693 studied in this work. The relative ratio of the detected species HOCN:HCOCN:HOCH₂CN is 2.8:1:1. By extrapolating the hydroxy/aldehyde (OH/HCO) ratio of HOCN/HCOCN to HOCH₂CN/HCOCH₂CN, one should expect an abundance of 0.15×10^{-10} for HCOCH₂CN, more than one order of magnitude lower than the upper limit derived from current observations ($< 2.7 \times 10^{-10}$, see Table 4). This suggests that deeper observations reaching higher sensitivity will be needed to address the detection of this species.

In the following, we discuss possible formation routes of the different O-bearing nitriles, combining the results obtained in G+0.693 and in other interstellar sources with theoretical and experimental works:

- **HOCN:** besides G+0.693, this species was detected previously towards several other positions of the Sgr B2 region in the Galactic Center (Brünken et al. 2009; Brünken et al. 2010), and towards several dense cores (B1-b, L1544, L183, L483) as well as the lukewarm corino L1527 (Marcelino et al. 2010; Marcelino et al. 2018). Figure 8 shows that the HOCN abundance derived in G+0.693 is of the same order of magnitude of those detected in other Sgr B2 positions ($\sim 10^{-11} - 10^{-10}$; Brünken et al. 2010), and higher than those derived in the dense cores and L1527 (Marcelino et al. 2018). This suggests that the role of

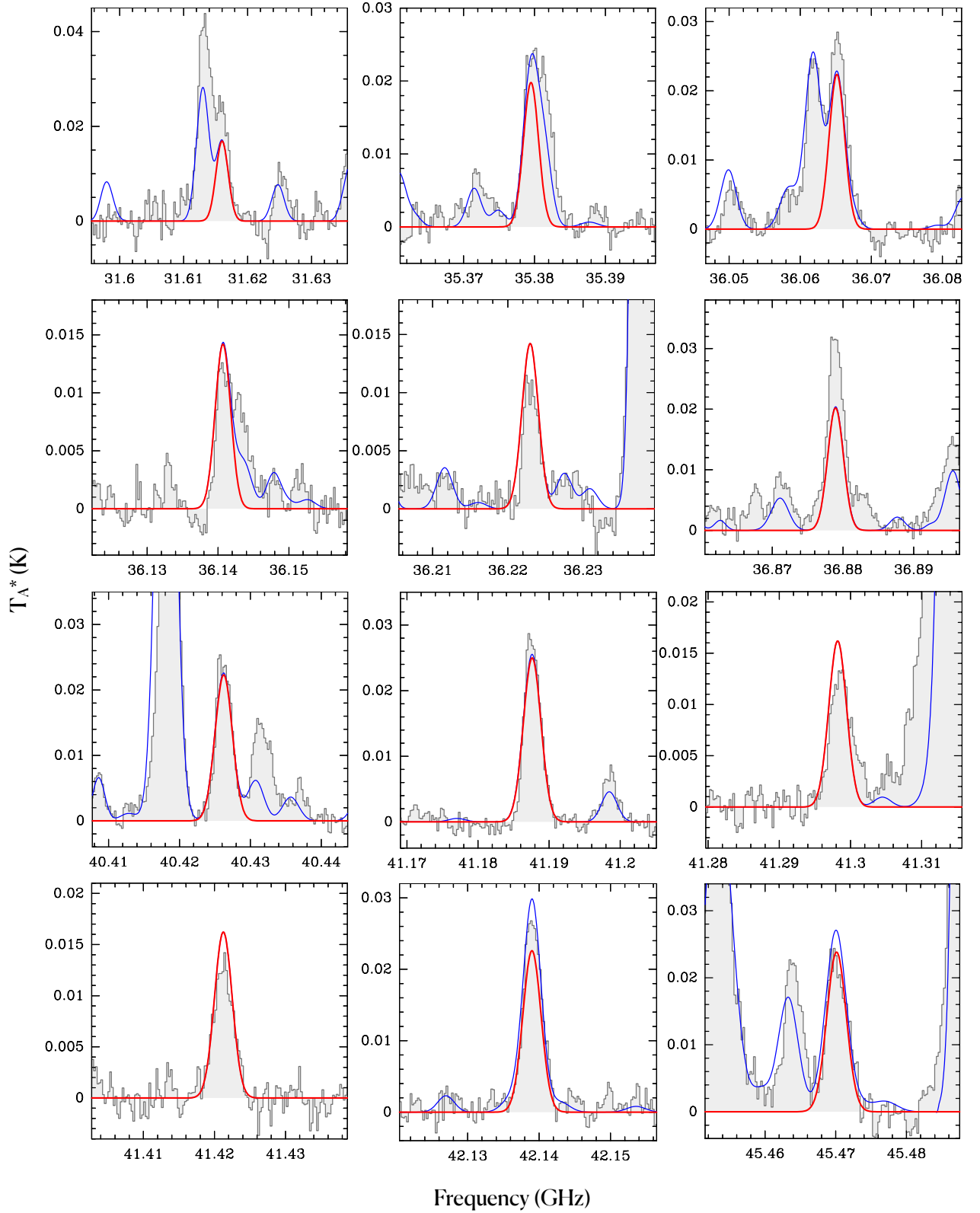


Figure 5. Selected transitions of cyanoallene (CH_2CCHCN ; see Table 3) detected towards the G+0.693 molecular cloud. The best LTE fit derived with MADCUBA for the CH_2CCHCN emission is shown with a red curve, while the blue curve shows the total emission considering all the species identified towards this molecular cloud. The y-axis shows the line intensity in antenna temperature scale (T_A^*) in Kelvin, and the x-axis shows the frequency in GHz.

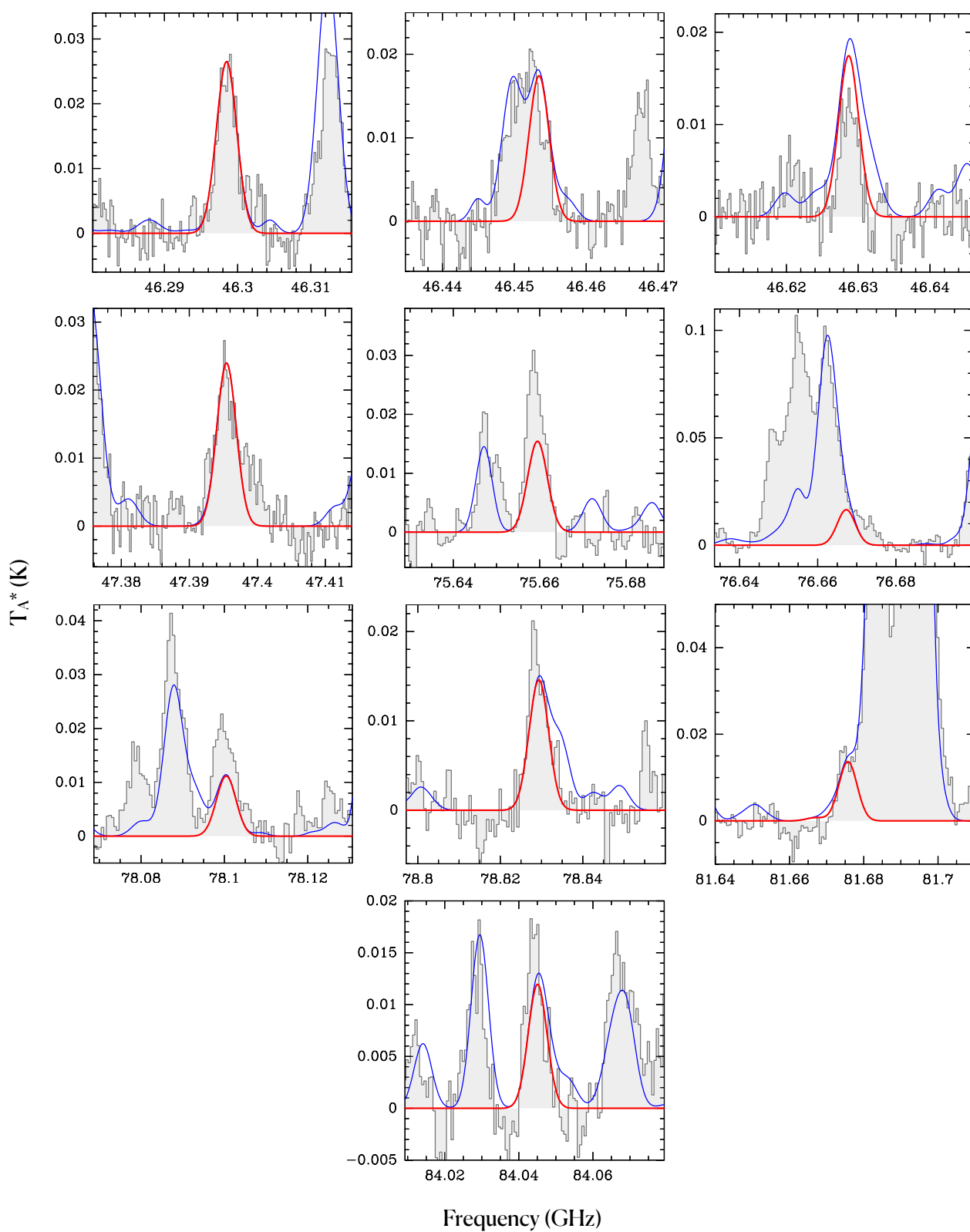


Figure 5. Continued.

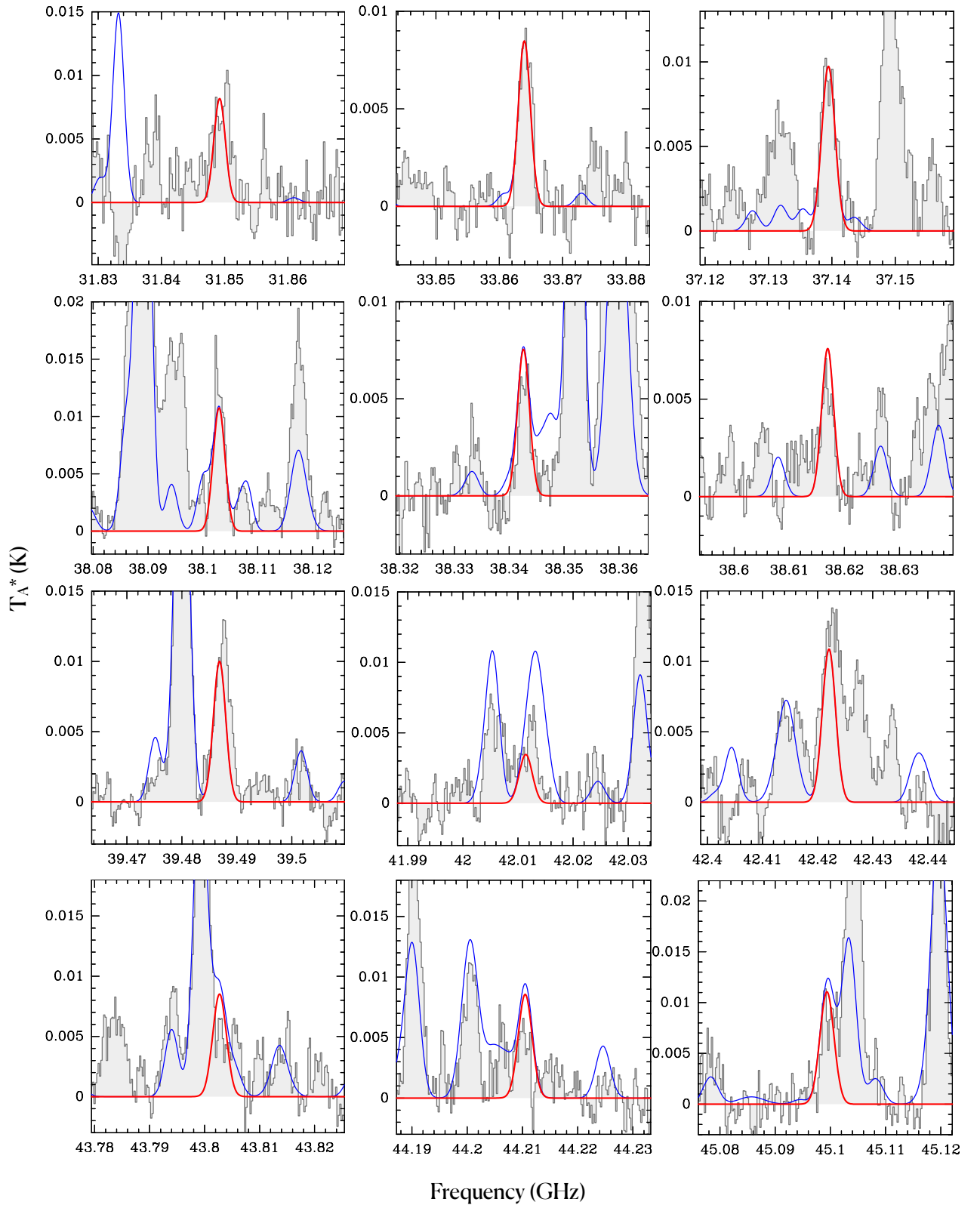


Figure 6. Selected transitions of propargyl cyanide (HCCCH_2CN ; see Table 3) detected towards the G+0.693 molecular cloud. The best LTE fit derived with MADCUBA for the HCCCH_2CN emission is shown with a red curve, while the blue curve shows the total emission considering all the species identified towards this molecular cloud. The y-axis shows the line intensity in antenna temperature scale (T_A^*) in Kelvin, and the x-axis shows the frequency in GHz.

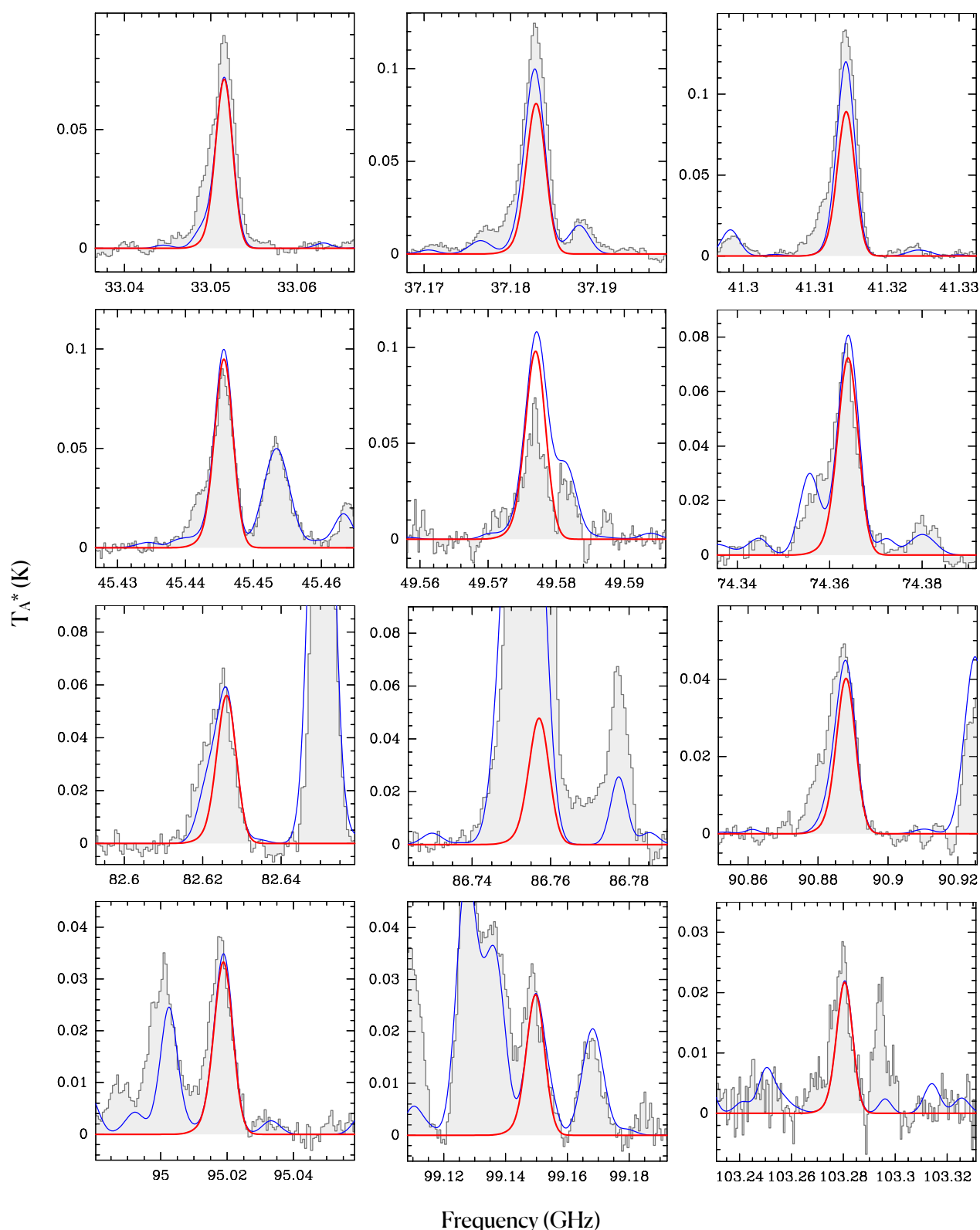


Figure 7. Selected transitions of cyanopropyne (CH_3CCCN ; see Table 3) detected towards the G+0.693 molecular cloud. The best LTE fit derived with MADCUBA for the CH_3CCCN emission is shown with a red curve, while the blue curve shows the total emission considering all the species identified towards this molecular cloud. The y-axis shows the line intensity in antenna temperature scale (T_A^*) in Kelvin, and the x-axis shows the frequency in GHz.

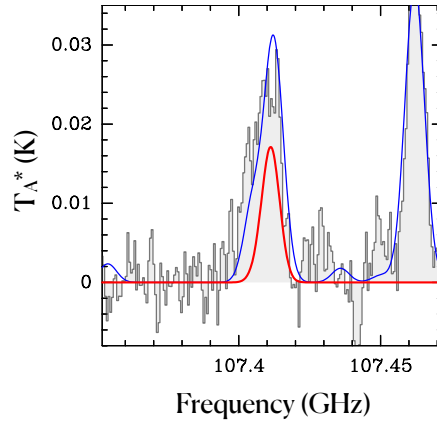


Figure 7. Continued.

Table 4. Derived physical parameters of the nitriles towards G+0.693 analysed in this work using MADCUBA, along with their associated uncertainties. The fixed parameters used in the fit are shown without associated uncertainties (see text).

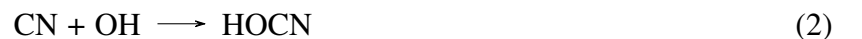
Molecule	N^a ($\times 10^{13} \text{ cm}^{-2}$)	T_{ex} (K)	v_{LSR} (km s^{-1})	FWHM (km s^{-1})	Abundance ^b ($\times 10^{-10}$)
HOCN	2.13 ± 0.04	7.4 ± 0.2	68.0 ± 0.2	19.2 ± 0.3	1.6
HCOCN	0.76 ± 0.11	7.4	68	19.2	0.6
HOCH ₂ CN	0.8 ± 0.2	7.4	67	19.2	0.6
HCOCH ₂ CN	< 3.6	7.4	67	19.2	< 2.7
CH ₂ CCHCN	2.34 ± 0.06	12.1 ± 0.5	66.1 ± 0.3	21.3 ± 0.7	1.7
HCCCH ₂ CN	1.77 ± 0.08	12.1	67.0 ± 0.6	21.3	1.3
CH ₃ CCCN	1.35 ± 0.03	18.6 ± 1.0	68	21.3	1.0

(a) The uncertainties of the column densities are derived by the AUTOFIT algorithm implemented in MADCUBA (see Martín et al. 2019 for details, and do not contain calibrations errors, which are expected to be $\sim 10\%$). (b) We adopted $N_{\text{H}_2} = 1.35 \times 10^{23} \text{ cm}^{-2}$, from Martín et al. (2008).

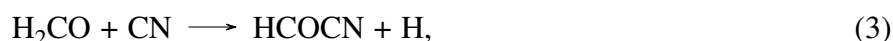
surface-chemistry and the presence of shocks enhance the HOCN abundance, similarly to its isomer HNCO (Hasegawa and Herbst 1993; Garrod et al. 2008; Martín et al. 2008; Rodríguez-Fernández et al. 2010; Quénard et al. 2018). The chemistry of the molecular clouds of the Galactic Center, and that of G+0.693 in particular, is dominated by large-scale shocks (Martín-Pintado et al. 2001; Martín et al. 2008), which are responsible for the sputtering of dust grains, releasing many molecules formed on the grain surfaces into the gas phase (see Caselli et al. 1997; Jiménez-Serra et al. 2008). This can increase the abundance of the species by orders of magnitude. Similarly to isomer HNCO, which is efficiently formed on grain surfaces by hydrogenation of accreted OCN (Hasegawa and Herbst 1993; Garrod et al. 2008), HOCN can also be formed on grain mantles if the oxygen atom is hydrogenated:



and then subsequently released by shocks (Brünken et al. 2010). An alternative surface route might be the reaction of two highly abundant species:



• **HCOCN:** this species has been detected previously in the massive hot core SgrB2 (N) (Remijan et al. 2008), and in the dark cloud TMC-1 (Cernicharo et al. 2021). The HCOCN abundances found in G+0.693 and TMC-1 are very similar, in the range of $(3.5-5) \times 10^{-11}$, as shown in Figure 8. These two regions have very different physical conditions, which imprint their chemistry. While in the case of the dark and cold TMC-1 cloud gas-phase chemistry is thought to be dominant, since thermal or shock-induced desorptions are highly unlikely, the chemistry of G+0.693 is strongly affected by shocks, and thus surface chemistry also plays an important role. Therefore, the similar HCOCN abundances in G+0.693 and TMC-1 points towards a predominant gas-phase chemistry origin. Indeed, the quantum chemical calculations by Tonolo et al. (2020) have shown that HCOCN species can be efficiently formed through the gas-phase reaction between formaldehyde (H_2CO) and the cyanide radical (CN), which are highly abundant species in the ISM, in which the CN radical attacks the unsaturated carbon of H_2CO and substitutes one of the H atoms:



• **HOCH₂CN:** this species was first detected in the ISM towards the hot corino IRAS 16293-2422 B (Zeng et al. 2019), and more recently towards the SMM1 hot corino in Serpens (Ligterink et al. 2021). The abundance derived in G+0.693 is 4.3×10^{-10} , very similar to that derived in the hot component of IRAS 16293-2422 B (Figure 8). The chemical model by Zeng et al. (2019) considered the surface formation route proposed by the laboratory experiments of Danger et al. (2012); Danger et al. (2013):



and ion-neutral destruction reactions with H_3^+ , HCO^+ , and H_3O^+ , and concluded that more chemical pathways are needed to explain the abundance observed in the hot corino IRAS 16293-2422 B. More recently, the quantum chemical cluster calculations performed by Woon (2021) have proposed new surface reactions between C^+ , which is distributed throughout the whole Galactic Center (Harris et al. 2021), and two very abundant species, HCN and HNC (e.g. Colzi et al. 2022), embedded in H_2O icy grain mantles. The C^+ ion reacts with HCN and HNC forming intermediate species that attacks neighboring H_2O molecules of the ices, resulting into the radicals HOCHNC and HOCHCN. These species can be easily hydrogenated on the grain surfaces to form HOCH_2CN . The inclusion of these alternative surface routes in the chemical models might help to explain the HOCH_2CN abundances detected in G+0.693 and hot corinos, where the molecules can be injected to the gas phase through shocks and thermal effects, respectively.

• **HCOCH₂CN:** the theoretical calculations performed by Horn et al. (2008) proposed that this species might be formed from two abundant precursors in the ISM:



However, while this reaction might occur in aqueous solution, its activation energy, 216 kJ mol^{-1} (25980 K), is too high to occur in the ISM. Recently, Alessandrini and Melosso (2021) have studied the reaction between oxirane (or ethylene oxide, $\text{c-C}_2\text{H}_4\text{O}$) –also detected towards G+0.693 (Requena-Torres et al. 2008) – and the CN radical. Although the main pathway is the H abstraction from oxirane, forming the oxiranyl radical, the formation of $\text{HCOCH}_2\text{CN} + \text{H}$ is also possible with a rate of $\sim 10^{-12} \text{ cm}^3 \text{ molec}^{-1} \text{ s}^{-1}$. New theoretical and/or experimental works of this species are needed to determine if it can be efficiently formed in the ISM, opening the possibility for its interstellar detection.

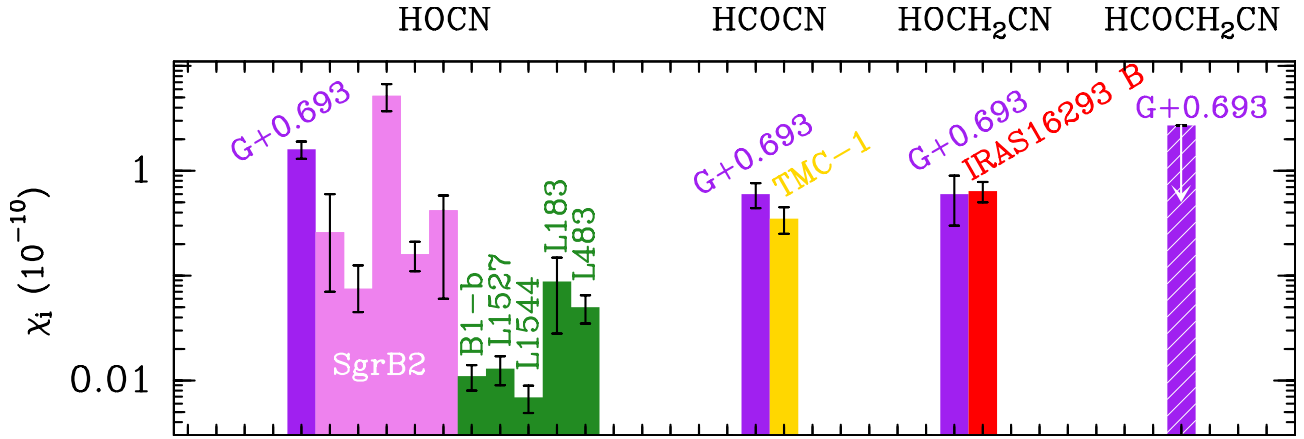
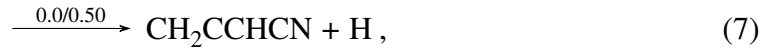


Figure 8. Molecular abundances with respect to H_2 of the oxygen-bearing nitriles studied in this work derived in different interstellar sources. Purple bars correspond to G+0.693 (this work; see Table 4), with the $HCOCH_2CN$ value indicating an upper limit. We compare with other sources: several positions also in the Sgr B2 region (magenta; Brünken et al. 2010, see also Marcelino et al. 2010); several dense cores (B1-b, L1544, L183, L483) and the lukewarm corino L1527 (green: Marcelino et al. 2010; Marcelino et al. 2018); the dark cloud TMC-1 (yellow; Cernicharo et al. 2021); and the IRAS 16293-2422 B hot corino (red, Zeng et al. 2019). To derive the uncertainties of the molecular abundances we have considered the uncertainties of the molecular column densities reported in the different works, or a 15% of the value of N if the uncertainty is not provided, and we assumed an uncertainty for the $N(H_2)$ column densities of 15%.

4.1.2 C_4H_3N isomers

The unsaturated C_4H_3N isomers towards G+0.693 have very similar abundances within a factor of 2, spanning a range of $(1.0-1.7) \times 10^{-10}$ (Table 4), as also previously observed in the dark cloud TMC-1 by Marcelino et al. (2021). Moreover, Figure 9 shows that the abundances in these two molecular clouds, which have very different physical conditions, as mentioned above, are very similar. This suggests that these molecules are predominantly formed through gas-phase chemistry (see previous discussion about HCOCN). Furthermore, since the three isomers are almost equally abundant, their respective formation might be linked to common precursors. Indeed, Balucani et al. (2000) proposed that these unsaturated nitriles can be formed efficiently by reactions in which the cyanide radical (CN) attacks an unsaturated carbon of the hydrocarbons methylacetylene (CH_3CCH) and allene (CH_2CCH_2):



in which the branching ratios for each reaction are indicated above each arrow (normalized to 1). These ratios were derived using the experiments and quantum chemical calculations by Abeysekera et al. (2015) / Balucani et al. (2000) in the first two reactions, and from Balucani et al. (2002) in the latter two reactions. These radical-neutral reactions show no entrance barriers, they have exit barriers well below the energy of the reactant molecules, and are exothermic. The proposed precursors CN and CH_3CCH are abundant molecules in the ISM. In particular, they were detected towards G+0.693 with molecular abundances of

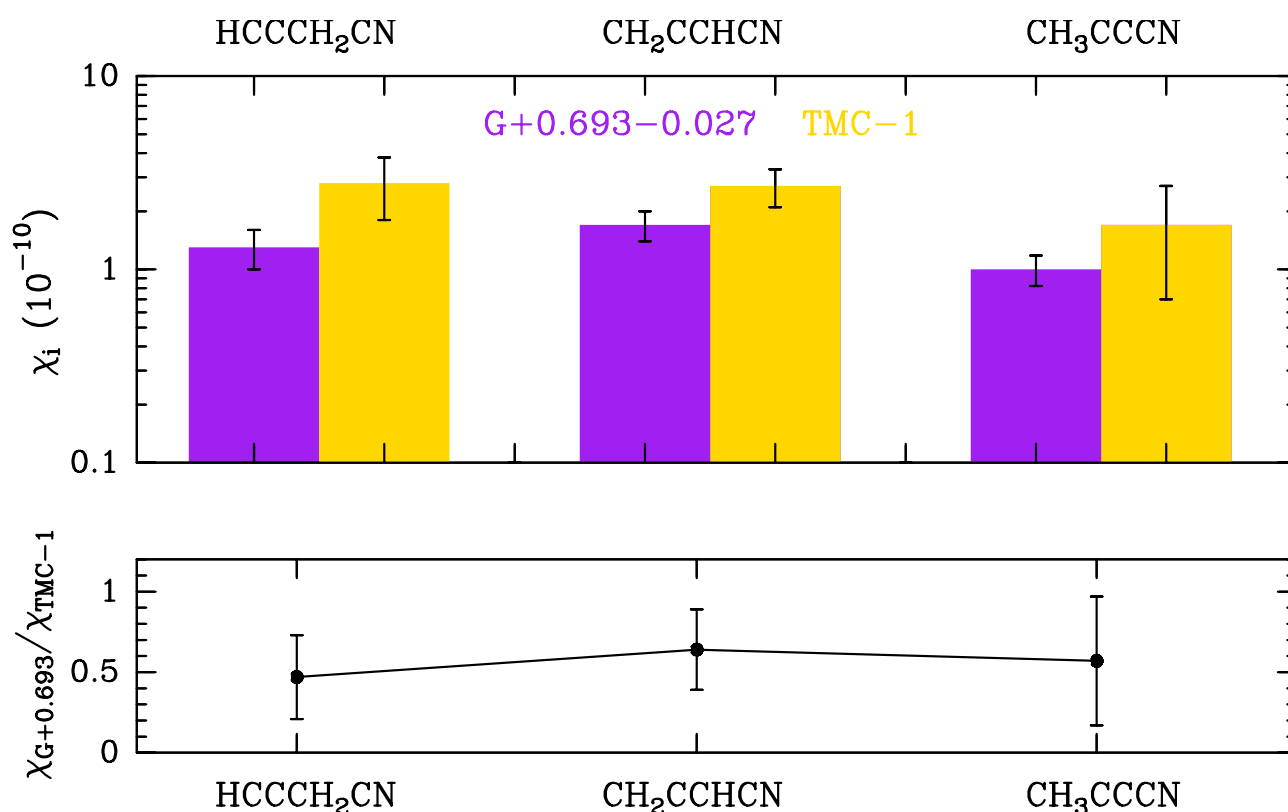


Figure 9. *Upper panel:* Abundances with respect to H_2 of the C_3H_4N isomers detected towards G+0.693 (purple; this work) and TMC-1 (yellow, Marcelino et al. 2021). To derive the uncertainties of the molecular abundances we have considered the uncertainties of the molecular column densities of the C_3H_4N isomers reported in this work (Table 4) and in Marcelino et al. 2021, and we assumed an uncertainty for the $N(H_2)$ column density of 15%. *Lower panel:* Molecular ratios between the abundances of the C_3H_4N isomers in G+0.693 and TMC-1.

1.5×10^{-8} and 1.3×10^{-8} , respectively (Rivilla et al. 2019a; Bizzocchi et al. 2020), so they are viable precursors. Allene (CH_2CCH_2) has zero dipole moment, so its detection through rotational spectroscopy is not possible, and thus its abundance is unknown. However, the similar abundances of the three isomers suggest that it can be as abundant as CH_3CCH in the ISM.

Regardless of the actual abundance of CH_2CCH_2 , which is unknown, the proposed branching ratios seem to be in conflict with the observational findings in G+0.693 and TMC-1, since they are not able to produce equal abundance for the three isomers. As already noted by Marcelino et al. (2021), it would be interesting to study the branching ratios of the $CH_2CHCH_2 + CN$ reaction using the chirped-pulse uniform flow experiment used by Abeysekera et al. (2015) for the $CH_2CCH + CN$ reaction, and compare them with the values derived from quantum chemical calculations by Balucani et al. (2002), to reconcile the experimental/theoretical works with the findings of the observations.

5 CONCLUSIONS: IMPLICATIONS FOR THE RNA-WORLD

Compounds of the nitrile family, under early Earth conditions, offer a rich chemistry due to the large number of reactions that they can trigger. Nitriles could be transformed into amides, carboxylic acids and esters via hydrolysis and alcoholysis respectively. Autocondensation of nitriles in a basic environment could yield to cyanoketones and cyanoenamines, a high reactive intermediate in the synthesis of complex

five- and six-member heterocycles (Erian 1993). The high amounts of ammonia of the reducing atmosphere of the primitive Earth is a favorable scenario to obtain amidines from nitriles (Shriner and Neumann 1944). Moreover, the NCN backbone of amidines offer an unique structure to yield complex N-containing heterocycles like purine and pyrimidine nucleobases. Furthermore, nitriles can activate the formation of the building blocks of RNA, ribonucleotides (e.g. Powner et al. 2009; Powner and Sutherland 2010; Patel et al. 2015). Two of the nitriles studied in this work, i.e. glycolonitrile and cyanoacetaldehyde, have been proposed as activation agents for the formation of more complex molecules with prebiotic relevance. The latter (HCOCH_2CN) is a precursor of cytosine (Robertson and Miller 1995; Nelson et al. 2001; Menor-Salván et al. 2009). The former (HOCH_2CN) is not only a fundamental precursor to ribonucleotides and lipids (Ritson and Sutherland 2012, 2013; Patel et al. 2015; Ritson et al. 2018; Liu et al. 2018), but also of other biologically-important molecules such as the simplest amino acid glycine ($\text{NH}_2\text{CH}_2\text{COOH}$; Rodriguez et al. 2019), and of the nucleobase adenine through rapid HCN oligomerisation (Schwartz and Goverde 1982; Menor-Salván and Marín-Yaseli 2012). Unsaturated carbon-chain nitriles like the $\text{C}_4\text{H}_3\text{N}$ isomers studied in this work are also especially interesting for prebiotic chemistry because the presence of unsaturated bonds allows further chemical evolution that can produce biomolecules (Rosi et al. 2018).

This work extends the repertoire of nitriles detected in the G+0.693 molecular cloud, a region that exhibits one of the richest chemical content in the ISM, and hence it is a well suited testbed to census the molecular species present in the ISM. Besides HOCN, already reported by Brünken et al. (2010) and Zeng et al. (2018), we have provided the tentative detections towards this source of HCOCN and HOCH_2CN (third detection in the ISM), and the detection of the three unsaturated $\text{C}_4\text{H}_3\text{N}$ isomers (being the second source after TMC-1 in which all three isomers are identified). These detections confirm the rich reservoir of nitriles in space, and complete the list of prebiotic molecular precursors detected previously, including species directly involved in the synthesis of ribonucleotides such as glycolaldehyde (HCOCH_2OH ; Hollis et al. 2004; Requena-Torres et al. 2006; Beltrán et al. 2009; Jørgensen et al. 2012), urea (Belloche et al. 2019; Jiménez-Serra et al. 2020), hydroxylamine NH_2OH (Rivilla et al. 2020), and 1,2-ethenediol (Rivilla et al. 2022a); of amino acids, such as amino acetonitrile ($\text{NH}_2\text{CH}_2\text{CN}$; Belloche et al. 2008; Melosso et al. 2020); and of lipids, such as ethanolamine ($\text{NH}_2\text{CH}_2\text{CH}_2\text{OH}$; Rivilla et al. 2021a), and propanol ($\text{CH}_3\text{CH}_2\text{CH}_2\text{OH}$; Jimenez-Serra et al. 2022; Belloche et al. 2022).

In star- and planet-forming regions, this chemical feedstock can be processed through circumstellar disks, and subsequently incorporated into planetesimals and objects like comets and asteroids. We know that our planet suffered a heavy bombardment of extraterrestrial bodies ~ 500 Myr after its formation (e.g. Marchi et al. 2014). Laboratory impact experiments have shown that a significant fraction of the molecules contained in comets and meteorites could have been delivered intact to the early Earth (Pierazzo and Chyba 1999; Bertrand et al. 2009; McCaffrey et al. 2014; Zellner et al. 2020; Todd and Öberg 2020). Once on the planetary surface, under the appropriate physical/chemical conditions, these molecules could have allowed the development of the prebiotic processes that led to the dawn of life on Earth.

CONFLICT OF INTEREST STATEMENT

The authors declare that the research was conducted in the absence of any commercial or financial relationships that could be construed as a potential conflict of interest.

AUTHOR CONTRIBUTIONS

V.M.R. initiated and led the project. V.M.R., J.M.-P., F.R.-V., B.T. and P.d.V. performed the observations. V.M.R., I.J.-S., and J.M.-P. performed the data reduction. V.M.R., L.C., S.Z., and I.J.S. contributed to the data analysis. L.B. and M.M. performed the calculations of the cyanoacetaldehyde spectroscopy. V.M.R.

wrote an initial draft of the article. All the authors, including J.G.dlC., S.M. and M.A.R.-T., participated in data interpretation and discussion.

FUNDING

V.M.R. acknowledges support from the Comunidad de Madrid through the Atracción de Talento Investigador Modalidad 1 (Doctores con experiencia) Grant (COOL:Cosmic Origins of Life; 2019-T1/TIC-15379), and from the Agencia Estatal de Investigación (AEI) through the Ramón y Cajal programme (grant RYC2020-029387-I). I.J.-S., J.M.-P and L.C. have received partial support from the Spanish State Research Agency (AEI) through project number PID2019-105552RB-C41. J.G.d.l.C. acknowledges the Spanish State Research Agency (AEI) through project number MDM-2017-0737 Unidad de Excelencia “María de Maeztu”—Centro de Astrobiología and the Spanish State Research Agency (AEI) for partial financial support through Project No. PID2019-105552RB-C41.

ACKNOWLEDGMENTS

We thank the two reviewers for providing very constructive and useful comments and suggestions, which contributed to improve our work. We also thank Dr. Rougal Ritson for interesting discussions about the relevance of nitriles in prebiotic chemistry. We are very grateful to the IRAM 30m and Yebes 40m telescope staff for their precious help during the different observing runs. IRAM is supported by the National Institute for Universe Sciences and Astronomy/National Center for Scientific Research (France), Max Planck Society for the Advancement of Science (Germany), and the National Geographic Institute (IGN) (Spain). The 40m radio telescope at Yebes Observatory is operated by the IGN, Ministerio de Transportes, Movilidad y Agenda Urbana. V.M.R. and L.C. have received funding from the Comunidad de Madrid through the Atracción de Talento Investigador (Doctores con experiencia) Grant (COOL: Cosmic Origins Of Life; 2019-T1/TIC-15379). L.C. has also received partial support from the Spanish State Research Agency (AEI; project number PID2019-105552RB-C41). P.d.V. and B.T. thank the support from the European Research Council (ERC Grant 610256: NANOCOSMOS) and from the Spanish Ministerio de Ciencia e Innovación (MICIU) through project PID2019-107115GB-C21. B.T. also acknowledges the Spanish MICIU for funding support from grant PID2019-106235GB-I00.

DATA AVAILABILITY STATEMENT

The data underlying this article will be shared on reasonable request to the corresponding author.

REFERENCES

- Abeysekera, C., Joalland, B., Ariyasingha, N., Zack, L. N., Sims, I. R., Field, R. W., et al. (2015). Product branching in the low temperature reaction of cn with propyne by chirped-pulse microwave spectroscopy in a uniform supersonic flow. *The Journal of Physical Chemistry Letters* 6, 1599–1604. doi:10.1021/acs.jpcllett.5b00519. PMID: 26263320
- Alessandrini, S. and Melosso, M. (2021). Fate of the gas-phase reaction between oxirane and the cn radical in interstellar conditions. *Frontiers in Astronomy and Space Sciences* 8. doi:10.3389/fspas.2021.754977
- Balucani, N., Asvany, O., Huang, L. C. L., Lee, Y. T., Kaiser, R. I., Osamura, Y., et al. (2000). Formation of nitriles in the interstellar medium via reactions of cyano radicals, CN(x 2σ+), with unsaturated hydrocarbons. *The Astrophysical Journal* 545, 892–906. doi:10.1086/317848
- Balucani, N., Asvany, O., Kaiser, R.-I., and Osamura, Y. (2002). Formation of three c4h3n isomers from the reaction of cn (x2σ+) with allene, h2ccch2 (xa1), and methylacetylene, ch3cch (x1a1): a combined crossed beam and ab initio study. *The Journal of Physical Chemistry A* 106, 4301–4311

- Becker, S., Feldmann, J., Wiedemann, S., Okamura, H., Schneider, C., Iwan, K., et al. (2019). Unified prebiotically plausible synthesis of pyrimidine and purine rna ribonucleotides. *Science* 366, 76–82. doi:10.1126/science.aax2747
- Belloche, A., Garrod, R. T., Müller, H. S. P., Menten, K. M., Medvedev, I., Thomas, J., et al. (2019). Re-exploring Molecular Complexity with ALMA (ReMoCA): interstellar detection of urea. *A&A* 628, A10. doi:10.1051/0004-6361/201935428
- Belloche, A., Garrod, R. T., Zingsheim, O., Müller, H. S. P., and Menten, K. M. (2022). Interstellar detection and chemical modeling of iso-propanol and its normal isomer. *arXiv e-prints*, arXiv:2204.09912
- Belloche, A., Menten, K. M., Comito, C., Müller, H. S. P., Schilke, P., Ott, J., et al. (2008). Detection of amino acetonitrile in Sgr B2(N). *Astronomy & Astrophysics* 482, 179–196. doi:10.1051/0004-6361:20079203
- Beltrán, M. T., Codella, C., Viti, S., Neri, R., and Cesaroni, R. (2009). First Detection of Glycolaldehyde Outside the Galactic Center. *The Astrophysical Journal Letters* 690, L93–L96. doi:10.1088/0004-637X/690/2/L93
- Bertrand, M., van der Gaast, S., Vilas, F., Hörz, F., Haynes, G., Chabin, A., et al. (2009). The fate of amino acids during simulated meteoritic impact. *Astrobiology* 9, 943–951. doi:10.1089/ast.2008.0327. PMID: 20041747
- Bester, M., Tanimoto, M., Vowinkel, B., Winnewisser, G., and Yamada, K. (1983). Rotational spectrum of methylcyanoacetylene a new millimeter wave spectrometer. *Zeitschrift für Naturforschung A* 38, 64–67. doi:doi:10.1515/zna-1983-0112
- Bester, M., Yamada, K., Winnewisser, G., Joentgen, W., Altenbach, H.-J., and Vogel, E. (1984). Millimeter wave spectrum of methyldiacetylene, $\text{CH}_3\text{C}_4\text{H}$. *Astronomy and Astrophysics* 137, L20–L22
- Bizzocchi, L., Prudenizano, D., Rivilla, V. M., Pietropolli-Charmet, A., Giuliano, B. M., Caselli, P., et al. (2020). Propargylimine in the laboratory and in space: millimetre-wave spectroscopy and its first detection in the ISM. *A&A* 640, A98. doi:10.1051/0004-6361/202038083
- Bogey, M., Demuynck, C., Destombes, J., and Vallee, Y. (1995). Millimeter-wave spectrum of formyl cyanide, HCOCN : Centrifugal distortion and hyperfine structure analysis. *Journal of Molecular Spectroscopy* 172, 344–351
- Bouchy, A., Demaison, J., Roussy, G., and Barriol, J. (1973). Microwave spectrum of cyanoallene. *Journal of Molecular Structure* 18, 211–217
- Brünken, S., Belloche, A., Martín, S., Verheyen, L., and Menten, K. M. (2010). Interstellar HOCN in the Galactic center region. *Astronomy & Astrophysics* 516, A109. doi:10.1051/0004-6361/200912456
- Brünken, S., Gottlieb, C., McCarthy, M., and Thaddeus, P. (2009). Laboratory detection of HOCN and tentative identification in sgr b2. *The Astrophysical Journal* 697, 880
- Canavelli, P., Islam, S., and Powner, M. W. (2019). Peptide ligation by chemoselective aminonitrile coupling in water. *Nature* 571, 546–549
- Caselli, P., Hartquist, T. W., and Havnes, O. (1997). Grain-grain collisions and sputtering in oblique C-type shocks. *A&A* 322, 296–301
- Cernicharo, J., Cabezas, C., Agúndez, M., Tercero, B., Pardo, J. R., Marcelino, N., et al. (2021). TMC-1, the starless core sulfur factory: Discovery of NCS, HCCS, H_2CCS , H_2CCCS , and C_4S and detection of C_5S . *A&A* 648, L3. doi:10.1051/0004-6361/202140642
- Chyba, C. and Sagan, C. (1992). Endogenous production, exogenous delivery and impact-shock synthesis of organic molecules: An inventory for the origins of life. *Nature* 355, 125–132. doi:10.1038/355125a0
- Colzi, L., Martín-Pintado, J., Rivilla, V. M., Jiménez-Serra, I., Zeng, S., Rodríguez-Almeida, L. F., et al. (2022). Deuterium Fractionation as a Multiphase Component Tracer in the Galactic Center. *ApJL* 926,

- L22. doi:10.3847/2041-8213/ac52ac
- Cooper, G., Kimmich, N., Belisle, W., Sarinana, J., Brabham, K., and Garrel, L. (2001). Carbonaceous meteorites as a source of sugar-related organic compounds for the early earth. *Nature* 414, 879–883
- Császár, A. G. (1989). Theoretical prediction of vibrational and rotational spectra. formyl cyanide, hcocn, and thioformyl cyanide, hcsn. *Chemical physics letters* 162, 361–368
- Danger, G., Duvernay, F., Theulé, P., Borget, F., and Chiavassa, T. (2012). Hydroxyacetonitrile (HOCH₂CN) Formation in Astrophysical Conditions. Competition with the Aminomethanol, a Glycine precursor. *ApJ* 756, 11. doi:10.1088/0004-637X/756/1/11
- Danger, G., Duvernay, F., Theulé, P., Borget, F., Guillemin, J.-C., and Chiavassa, T. (2013). Hydroxyacetonitrile (HOCH₂cn) as a precursor for formylcyanide (CHOCN), ketenimine (CH₂cnh), and cyanogen (NCCN) in astrophysical conditions. *Astronomy and Astrophysics* 549, A93. doi:10.1051/0004-6361/201219779
- Demaison, J., Pohl, I., and Rudolph, H. (1985). Millimeter-wave spectrum of 3-butyne nitrile: Dipole moment and centrifugal distortion constants. *Journal of Molecular Spectroscopy* 114, 210–218
- Endres, C. P., Schlemmer, S., Schilke, P., Stutzki, J., and Müller, H. S. P. (2016). The Cologne Database for Molecular Spectroscopy, CDMS, in the Virtual Atomic and Molecular Data Centre, VAMDC. *Journal of Molecular Spectroscopy* 327, 95–104. doi:10.1016/j.jms.2016.03.005
- Erian, A. W. (1993). The chemistry of .beta.-enaminonitriles as versatile reagents in heterocyclic synthesis. *Chemical Reviews* 93, 1991–2005. doi:10.1021/cr00022a002
- Foden, C. S., Islam, S., Fernández-García, C., Maugeri, L., Sheppard, T. D., and Powner, M. W. (2020). Prebiotic synthesis of cysteine peptides that catalyze peptide ligation in neutral water. *Science* 370, 865–869
- Garrod, R. T., Widicus Weaver, S. L., and Herbst, E. (2008). Complex Chemistry in Star-forming Regions: An Expanded Gas-Grain Warm-up Chemical Model. *The Astrophysical Journal* 682, 283–302. doi:10.1086/588035
- Gilbert, W. (1986). Origin of life: The RNA world. *Nature* 319, 618. doi:10.1038/319618a0
- Harris, A. I., Güsten, R., Requena-Torres, M. A., Riquelme, D., Morris, M. R., Stacey, G. J., et al. (2021). SOFIA-upGREAT Imaging Spectroscopy of the [C II] 158 μ m Fine-structure Line of the Sgr B Region in the Galactic Center. *ApJ* 921, 33. doi:10.3847/1538-4357/ac1863
- Hasegawa, T. I. and Herbst, E. (1993). New gas–grain chemical models of quiescent dense interstellar clouds: the effects of h₂ tunnelling reactions and cosmic ray induced desorption. *Monthly Notices of the Royal Astronomical Society* 261, 83–102
- Hollis, J. M., Jewell, P. R., Lovas, F. J., and Remijan, A. (2004). Green Bank Telescope Observations of Interstellar Glycolaldehyde: Low-Temperature Sugar. *ApJL* 613, L45–L48. doi:10.1086/424927
- Horn, A., Møllendal, H., and Guillemin, J.-C. (2008). A Quantum Chemical Study of the Generation of a Potential Prebiotic Compound, Cyanoacetaldehyde, and Related Sulfur Containing Species. *Journal of Physical Chemistry A* 112, 11009–11016. doi:10.1021/jp805357w
- Jiménez-Serra, I., Caselli, P., Martín-Pintado, J., and Hartquist, T. W. (2008). Parametrization of C-shocks. Evolution of the sputtering of grains. *A&A* 482, 549–559. doi:10.1051/0004-6361:20078054
- Jiménez-Serra, I., Martín-Pintado, J., Rivilla, V. M., Rodríguez-Almeida, L., Alonso, E. R., Zeng, S., et al. (2020). Toward the RNA-World in the Interstellar Medium—Detection of Urea and Search of 2-Amino-oxazole and Simple Sugars. *Astrobiology* 20, 1048–1066. doi:10.1089/ast.2019.2125
- Jimenez-Serra, I., Rodriguez-Almeida, L. F., Martin-Pintado, J., Rivilla, V. M., Melosso, M., Zeng, S., et al. (2022). Precursors of fatty alcohols in the ISM: Discovery of n-propanol. *arXiv e-prints*, arXiv:2204.08267

- Jørgensen, J. K., Favre, C., Bisschop, S. E., Bourke, T. L., van Dishoeck, E. F., and Schmalzl, M. (2012). Detection of the Simplest Sugar, Glycolaldehyde, in a Solar-type Protostar with ALMA. *ApJL* 757, L4. doi:10.1088/2041-8205/757/1/L4
- Ligterink, N. F. W., Ahmadi, A., Coutens, A., Tychoniec, Ł., Calcutt, H., van Dishoeck, E. F., et al. (2021). The prebiotic molecular inventory of Serpens SMM1. I. An investigation of the isomers CH₃NCO and HOCH₂CN. *A&A* 647, A87. doi:10.1051/0004-6361/202039619
- Liu, Z., Mariani, A., Wu, L., Ritson, D., Folli, A., Murphy, D., et al. (2018). Tuning the reactivity of nitriles using cu (ii) catalysis—potentially prebiotic activation of nucleotides. *Chemical science* 9, 7053–7057
- Lovas, F. J., Remijan, A. J., Hollis, J., Jewell, P., and Snyder, L. E. (2006). Hyperfine structure identification of interstellar cyanoallene toward tmc-1. *The Astrophysical Journal Letters* 637, L37
- Marcelino, N., Agúndez, M., Cernicharo, J., Roueff, E., and Tafalla, M. (2018). Discovery of the elusive radical NCO and confirmation of H₂NCO⁺ in space. *A&A* 612, L10. doi:10.1051/0004-6361/201833074
- Marcelino, N., Brünken, S., Cernicharo, J., Quan, D., Roueff, E., Herbst, E., et al. (2010). The puzzling behavior of HNCO isomers in molecular clouds. *Astronomy and Astrophysics* 516, A105. doi:10.1051/0004-6361/200913806
- Marcelino, N., Tercero, B., Agúndez, M., and Cernicharo, J. (2021). A study of C₄H₃N isomers in TMC-1: Line by line detection of HCCCH₂CN. *A&A* 646, L9. doi:10.1051/0004-6361/202040177
- Marchi, S., Bottke, W., Elkins-Tanton, L., Bierhaus, M., Wuennemann, K., Morbidelli, A., et al. (2014). Widespread mixing and burial of earth's hadean crust by asteroid impacts. *Nature* 511, 578–582
- Margulès, L., McGuire, B. A., Senent, M. L., Motiyenko, R. A., Remijan, A., and Guillemin, J. C. (2017). Submillimeter spectra of 2-hydroxyacetonitrile (glycolonitrile; HOCH₂cn) and its searches in GBT PRIMOS observations of Sgr B2(N). *Astronomy & Astrophysics* 601, A50. doi:10.1051/0004-6361/201628551
- Mariani, A., Russell, D. A., Javelle, T., and Sutherland, J. D. (2018). A light-releasable potentially prebiotic nucleotide activating agent. *Journal of the American Chemical Society* 140, 8657–8661
- Martín, S., Martín-Pintado, J., Blanco-Sánchez, C., Rivilla, V. M., Rodríguez-Franco, A., and Rico-Villas, F. (2019). Spectral Line Identification and Modelling (SLIM) in the MADrid Data CUBe Analysis (MADCUBA) package. Interactive software for data cube analysis. *A&A* 631, A159. doi:10.1051/0004-6361/201936144
- Martín, S., Requena-Torres, M. A., Martín-Pintado, J., and Mauersberger, R. (2008). Tracing shocks and photodissociation in the Galactic center region. *The Astrophysical Journal* 678, 245–254. doi:10.1086/533409. ArXiv: 0801.3614
- Martín-Pintado, J., Rizzo, J. R., de Vicente, P., Rodríguez-Fernández, N. J., and Fuente, A. (2001). Large-Scale Grain Mantle Disruption in the Galactic Center. *ApJL* 548, L65–L68. doi:10.1086/318937
- McCaffrey, V., Zellner, N., Waun, C., Bennett, E., and Earl, E. (2014). Reactivity and survivability of glycolaldehyde in simulated meteorite impact experiments. *Origins of Life and Evolution of Biospheres* 44, 29–42
- McGuire, B. A., Burkhardt, A. M., Loomis, R. A., Shingledecker, C. N., Lee, K. L. K., Charnley, S. B., et al. (2020). Early science from gotham: project overview, methods, and the detection of interstellar propargyl cyanide (hccch₂cn) in tmc-1. *The Astrophysical Journal Letters* 900, L10
- Melosso, M., Belloche, A., Martin-Drumel, M. A., Piralì, O., Tamassia, F., Bizzocchi, L., et al. (2020). Far-infrared laboratory spectroscopy of aminoacetonitrile and first interstellar detection of its vibrationally excited transitions. *A&A* 641, A160. doi:10.1051/0004-6361/202038466
- Menor Salván, C., Bouza, M., Fialho, D. M., Burcar, B. T., Fernández, F. M., and Hud, N. V. (2020). Prebiotic origin of pre-rna building blocks in a urea “warm little pond” scenario. *ChemBioChem* 21,

3504–3510

- Menor-Salván, C. and Marín-Yaseli, M. R. (2012). Prebiotic chemistry in eutectic solutions at the water–ice matrix. *Chemical Society Reviews* 41, 5404–5415
- Menor-Salván, C., Ruiz-Bermejo, D. M., Guzmán, M. I., Osuna-Esteban, S., and Veintemillas-Verdaguer, S. (2009). Synthesis of pyrimidines and triazines in ice: Implications for the prebiotic chemistry of nucleobases. *Chemistry—A European Journal* 15, 4411–4418
- Moïses, A., Boucher, D., Burie, J., Demaison, J., and Dubrulle, A. (1982). Millimeter-wave spectrum of methylcyanoacetylene. *Journal of Molecular Spectroscopy* 92, 497–498
- Møllendal, H., Margulès, L., Motiyenko, R. A., Larsen, N. W., and Guillemin, J.-C. (2012). Rotational Spectrum and Conformational Composition of Cyanoacetaldehyde, a Compound of Potential Prebiotic and Astrochemical Interest. *Journal of Physical Chemistry A* 116, 4047–4056. doi:10.1021/jp212306z
- Nelson, K. E., Robertson, M. P., Levy, M., and Miller, S. L. (2001). Concentration by evaporation and the prebiotic synthesis of cytosine. *Origins of Life and Evolution of the Biosphere* 31, 221–229
- Oró, J. (1961). Mechanism of Synthesis of Adenine from Hydrogen Cyanide under Possible Primitive Earth Conditions. *Nature* 191, 1193–1194. doi:10.1038/1911193a0
- Patel, B. H., Percivalle, C., Ritson, D. J., Duffy, C. D., and Sutherland, J. D. (2015). Common origins of RNA, protein and lipid precursors in a cyanosulfidic protometabolism. *Nature Chemistry* 7, 301–307. doi:10.1038/nchem.2202
- Pearce, B. K., Tupper, A. S., Pudritz, R. E., and Higgs, P. G. (2018). Constraining the time interval for the origin of life on earth. *Astrobiology* 18, 343–364. doi:10.1089/ast.2017.1674. PMID: 29570409
- Pickett, H. M. (1991). The fitting and prediction of vibration-rotation spectra with spin interactions. *Journal of Molecular Spectroscopy* 148, 371–377. doi:10.1016/0022-2852(91)90393-O
- Pickett, H. M., Poynter, R. L., Cohen, E. A., Delitsky, M. L., Pearson, J. C., and Müller, H. S. P. (1998). Submillimeter, millimeter and microwave spectral line catalog. *JQSRT* 60, 883–890. doi:10.1016/S0022-4073(98)00091-0
- Pierazzo, E. and Chyba, C. F. (1999). Amino acid survival in large cometary impacts. *Meteoritics & Planetary Science* 34, 909–918. doi:10.1111/j.1945-5100.1999.tb01409.x
- Powner, M. and Sutherland, J. (2010). Phosphate-mediated interconversion of ribo- and arabino-configured prebiotic nucleotide intermediates. *Angewandte Chemie International Edition* 49, 4641–4643. doi:https://doi.org/10.1002/anie.201001662
- Powner, M. W., Gerland, B., and Sutherland, J. D. (2009). Synthesis of activated pyrimidine ribonucleotides in prebiotically plausible conditions. *Nature* 459, 239–242. doi:10.1038/nature08013
- Quénard, D., Jiménez-Serra, I., Viti, S., Holdship, J., and Coutens, A. (2018). Chemical modelling of complex organic molecules with peptide-like bonds in star-forming regions. *Monthly Notices of the Royal Astronomical Society* 474, 2796–2812. doi:10.1093/mnras/stx2960
- Remijan, A. J., Hollis, J. M., Lovas, F. J., Stork, W. D., Jewell, P. R., and Meier, D. S. (2008). Detection of Interstellar Cyanoformaldehyde (CNCHO). *The Astrophysical Journal Letters* 675, L85. doi:10.1086/533529
- Requena-Torres, M. A., Martín-Pintado, J., Martín, S., and Morris, M. R. (2008). The largest oxygen bearing organic molecule repository. *The Astrophysical Journal* 672, 352–360. doi:10.1086/523627. ArXiv: 0709.0542
- Requena-Torres, M. A., Martín-Pintado, J., Rodríguez-Franco, A., Martín, S., Rodríguez-Fernández, N. J., and de Vicente, P. (2006). Organic Molecules in the Galactic Center. Hot Core Chemistry without Hot Cores. *Astronomy & Astrophysics* 455, 971–985. doi:10.1051/0004-6361:20065190. ArXiv: astro-ph/0605031

- Ritson, D. and Sutherland, J. D. (2012). Prebiotic synthesis of simple sugars by photoredox systems chemistry. *Nature chemistry* 4, 895–899
- Ritson, D. J., Battilocchio, C., Ley, S. V., and Sutherland, J. D. (2018). Mimicking the surface and prebiotic chemistry of early earth using flow chemistry. *Nature communications* 9, 1–10
- Ritson, D. J. and Sutherland, J. D. (2013). Synthesis of aldehydic ribonucleotide and amino acid precursors by photoredox chemistry. *Angewandte Chemie International Edition* 52, 5845–5847. doi:https://doi.org/10.1002/anie.201300321
- Rivilla, V. M., Beltrán, M. T., Vasyunin, A., Caselli, P., Viti, S., Fontani, F., et al. (2019a). First ALMA maps of HCO, an important precursor of complex organic molecules, towards IRAS 16293-2422. *MNRAS* 483, 806–823. doi:10.1093/mnras/sty3078
- Rivilla, V. M., Colzi, L., Jiménez-Serra, I., Martín-Pintado, J., Megías, A., Melosso, M., et al. (2022a). Precursors of the RNA World in Space: Detection of (Z)-1,2-ethenediol in the Interstellar Medium, a Key Intermediate in Sugar Formation. *ApJL* 929, L11. doi:10.3847/2041-8213/ac6186
- Rivilla, V. M., García De La Concepción, J., Jiménez-Serra, I., Martín-Pintado, J., Colzi, L., Tercero, B., et al. (2022b). Ionize Hard: Interstellar PO⁺ Detection. *Frontiers in Astronomy and Space Sciences* 9, 829288. doi:10.3389/fspas.2022.829288
- Rivilla, V. M., Jiménez-Serra, I., García de la Concepción, J., Martín-Pintado, J., Colzi, L., Rodríguez-Almeida, L. F., et al. (2021b). Detection of the cyanomethyl radical (HNCN): a new interstellar species with the NCN backbone. *MNRAS* 506, L79–L84. doi:10.1093/mnras/lsab074
- Rivilla, V. M., Jiménez-Serra, I., Martín-Pintado, J., Briones, C., Rodríguez-Almeida, L. F., Rico-Villas, F., et al. (2021a). Discovery in space of ethanolamine, the simplest phospholipid head group. *Proceedings of the National Academy of Science* 118, e2101314118. doi:10.1073/pnas.2101314118
- Rivilla, V. M., Martín-Pintado, J., Jiménez-Serra, I., Martín, S., Rodríguez-Almeida, L. F., Requena-Torres, M. A., et al. (2020). Prebiotic Precursors of the Primordial RNA World in Space: Detection of NH₂OH. *ApJL* 899, L28. doi:10.3847/2041-8213/abac55
- Rivilla, V. M., Martín-Pintado, J., Jiménez-Serra, I., Zeng, S., Martín, S., Armijos-Abendaño, J., et al. (2019b). Abundant Z-cyanomethanimine in the interstellar medium: paving the way to the synthesis of adenine. *MNRAS* 483, L114–L119. doi:10.1093/mnras/sly228
- Robertson, M. P. and Miller, S. L. (1995). An efficient prebiotic synthesis of cytosine and uracil. *Nature* 375, 772–774
- Rodríguez, L. E., House, C. H., Smith, K. E., Roberts, M. R., and Callahan, M. P. (2019). Nitrogen heterocycles form peptide nucleic acid precursors in complex prebiotic mixtures. *Scientific reports* 9, 1–12
- Rodríguez-Almeida, L. F., Jiménez-Serra, I., Rivilla, V. M., Martín-Pintado, J., Zeng, S., Tercero, B., et al. (2021a). Thiols in the Interstellar Medium: First Detection of HC(O)SH and Confirmation of C₂H₅SH. *ApJL* 912, L11. doi:10.3847/2041-8213/abf7cb
- Rodríguez-Almeida, L. F., Rivilla, V. M., Jiménez-Serra, I., Melosso, M., Colzi, L., Zeng, S., et al. (2021b). First detection of C₂H₅NCO in the ISM and search of other isocyanates towards the G+0.693-0.027 molecular cloud. *A&A* 654, L1. doi:10.1051/0004-6361/202141989
- Rodríguez-Fernández, N. J., Tafalla, M., Gueth, F., and Bachiller, R. (2010). HNCO enhancement by shocks in the L1157 molecular outflow. *A&A* 516, A98. doi:10.1051/0004-6361/201013997
- Rosi, M., Skouteris, D., Casavecchia, P., Falcinelli, S., Ceccarelli, C., and Balucani, N. (2018). Formation of nitrogen-bearing organic molecules in the reaction nh⁺ + c 2 h 5: A theoretical investigation and main implications for prebiotic chemistry in space. In *International conference on computational science and its applications* (Springer), 773–782

- Schwahn, G., Schieder, R., Bester, M., and Winnewisser, G. (1986). The millimeter wave spectrum of cyanoallene, $\text{CH}_2=\text{C}=\text{CH}=\text{CN}$, using a new digital lock-in technique. *Journal of molecular spectroscopy* 116, 263–270.
- Schwartz, A. W. and Goverde, M. (1982). Acceleration of hcn oligomerization by formaldehyde and related compounds: implications for prebiotic syntheses. *Journal of molecular evolution* 18, 351–353.
- Shriner, R. L. and Neumann, F. W. (1944). The chemistry of the amidines. *Chemical Reviews* 35, 351–425. doi:10.1021/cr60112a002
- Tercero, F., López-Pérez, J. A., Gallego, J. D., Beltrán, F., García, O., Patino-Esteban, M., et al. (2021). Yebes 40 m radio telescope and the broad band Nanocosmos receivers at 7 mm and 3 mm for line surveys. *A&A* 645, A37. doi:10.1051/0004-6361/202038701
- Todd, Z. R. and Öberg, K. I. (2020). Cometary delivery of hydrogen cyanide to the early earth. *Astrobiology* 20, 1109–1120.
- Tonolo, F., Lupi, J., Puzzarini, C., and Barone, V. (2020). The quest for a plausible formation route of formyl cyanide in the interstellar medium: a state-of-the-art quantum-chemical and kinetic approach. *The Astrophysical Journal* 900, 85. doi:10.3847/1538-4357/aba628
- Turner, B. E. (1971). Detection of Interstellar Cyanoacetylene. *ApJL* 163, L35. doi:10.1086/180662
- Turner, B. E., Liszt, H. S., Kaifu, N., and Kisliakov, A. G. (1975). Microwave detection of interstellar cyanamide. *The Astrophysical Journal Letters* 201, L149–L152. doi:10.1086/181963
- Woon, D. E. (2021). The Formation of Glycolonitrile (HOCH_2CN) from Reactions of C^+ with HCN and HNC on Icy Grain Mantles. *ApJ* 906, 20. doi:10.3847/1538-4357/abc691
- Zellner, N. E., McCaffrey, V. P., and Butler, J. H. (2020). Cometary glycolaldehyde as a source of pre-rna molecules. *Astrobiology* 20, 1377–1388. doi:10.1089/ast.2020.2216. PMID: 32985898
- Zeng, S., Jiménez-Serra, I., Rivilla, V. M., Martín, S., Martín-Pintado, J., Requena-Torres, M. A., et al. (2018). Complex organic molecules in the Galactic Centre: the N-bearing family. *Monthly Notices of the Royal Astronomical Society* 478, 2962–2975. doi:10.1093/mnras/sty1174
- Zeng, S., Jiménez-Serra, I., Rivilla, V. M., Martín-Pintado, J., Rodríguez-Almeida, L. F., Tercero, B., et al. (2021). Probing the Chemical Complexity of Amines in the ISM: Detection of Vinylamine ($\text{C}_2\text{H}_3\text{NH}_2$) and Tentative Detection of Ethylamine ($\text{C}_2\text{H}_5\text{NH}_2$). *ApJL* 920, L27. doi:10.3847/2041-8213/ac2c7e
- Zeng, S., Quénard, D., Jiménez-Serra, I., Martín-Pintado, J., Rivilla, V. M., Testi, L., et al. (2019). First detection of the pre-biotic molecule glycolonitrile (HOCH_2CN) in the interstellar medium. *MNRAS* 484, L43–L48. doi:10.1093/mnras/slz002
- Zeng, S., Zhang, Q., Jiménez-Serra, I., Tercero, B., Lu, X., Martín-Pintado, J., et al. (2020). Cloud-cloud collision as drivers of the chemical complexity in Galactic Centre molecular clouds. *MNRAS* 497, 4896–4909. doi:10.1093/mnras/staa2187